synthesized RNA was used for each electroporation. Trypsinized HuH-7 cells or Huh-7.5.1 cells (3×10^6 cells) were washed with Opti-MEM I (Invitrogen, Carlsbad, CA) and resuspended in Cytomix buffer [19]. RNA was then combined with 400 µl of cell suspension and the mixture was transferred to an electroporation cuvette (Bio-Rad, Hercules, CA). The cells were then pulsed at 260 V and 950 µF using the Gene Pulser II apparatus (Bio-Rad). Transfected cells were immediately transferred to 6-well plates containing culture medium and incubated at 37°C under standard 5% CO_2 conditions.

Luciferase reporter assay

Luciferase activity of the JFH-1 subgenomic replicon and chimeras in HuH-7 cells were measured as described previously [12,20]. Briefly, 5 µg of transcribed RNA was transfected into 3×10^6 HuH-7 cells by electroporation. Transfected cells were immediately resuspended in culture medium and seeded into 6-well culture plates. Cells were then harvested at 4, 24, and 48 h after transfection and lysed with 200 µl of Cell Culture Lysis Reagent (Promega, Madison, WI). Debris was removed by centrifugation. Luciferase activity was quantified using a Lumat LB9507 luminometer (EG & G Berthold, Bad Wildbad, Germany) and a Luciferase Assay System (Promega). Assays were performed three times independently, with each value corrected for transfection efficiency as determined by measuring luciferase activity 4 h after transfection. Data are presented as relative light units (RLU).

Quantification of HCV core protein

To estimate the concentration of HCV core protein in the culture medium, we harvested supernatants at the indicated time points. The supernatant was then passed through a filter with a 0.22- µm pore size (Millipore, Bedford, MA) and subjected to the chemiluminescence enzyme immunoassay (Lumipulse II HCV core assay, Fujirebio, Tokyo, Japan) in accordance with the manufacturer's instructions.

Infection of cells with secreted HCV and determination of infectivity

Culture medium from RNA transfected cells was collected at 72 hours post-transfection. Huh7.5.1 cells were seeded at a density of 1×10^4 cells per well in poly-*D*-lysine coated 96-well plates (CORNING, Corning, NY). On the following day, the collected culture media were serially diluted and used for inoculation of the seeded cells, and the plates were incubated for another 3 days at 37°C. The cells were fixed in methanol for 15 min at −20°C, and the infected foci were visualized by immunofluorescence as described below.

Cells were blocked for 1 hour with BlockAce (Dainippon Sumitomo Pharma, Osaka, Japan), then washed with PBS, followed by incubation with anti-core antibody at 50 µg/ml in BlockAce. After incubation for 1 hour at room temperature, the cells were washed and incubated with a 1:400 dilution of AlexaFluor 488-conjugated anti-mouse IgG (Molecular Probes, Eugene, OR) in BlockAce. The cells were then washed and examined using fluorescence microscopy (Olympus, Tokyo, Japan). Infectivity was quantified by counting the infected foci and expressed as focus forming units per milliliter (ffu/ml).

Chemicals and radio isotope

Nucleotides were purchased from GE, [α-^{32}P]UTP from New England Nuclear (Boston, MA), and human placental RNase inhibitor and restriction enzymes from TaKaRa (Shiga, Japan).

Statistical analysis

Significant differences were evaluated using the Student's *t*-test. $p<0.05$ was considered significant.

RNA secondary structure prediction

RNA secondary structure prediction was performed using Mfold software [21].

Results

As we have reported previously, the NS3 helicase and the NS5B-to-3′X regions of JFH-1 are important to confer replication competence to J6CF, a replication-incompetent strain [12]. Of these two regions, NS5B-to-3′X of JFH-1 is the most important to replication-competence. The NS5B region encodes RdRP, and the JFH-1-version of this polymerase may have high activity and be crucial to replication-competence. The requirement of 3′UTR of JFH-1 suggested that the RNA structure in this region is important for efficient genome replication. To understand the mechanisms of efficient replication of JFH-1 in HuH-7 cells, we focused on the NS5B-to-3′X region because the NS3 helicase region of JFH-1 had relatively minor effects on replication of J6CF derivatives [12]. In order to identify the important protein domains within RdRP required for efficient virus replication, we compared the RNA polymerase activity of HCV J6CF RdRP to that of JFH-1 RdRP using three assays, *in vitro* transcription with purified RdRP, *in vivo* virus RNA replication, and *in vivo* virus production. To identify the important sequences or structures in the NS5B-to-3′X region involved in efficient replication, we analyzed the effect of sequence differences in this region on replication of the viral genome.

Comparison of RNA polymerase activity *in vitro*

By comparing the sequence of RdRP of JFH-1 (GenBank Accession No. AB047639), J6CF (AF177036), other 2a strains (AB047640 – 5, AY746460, AF238481 - 5, AF169002 -5), a 1a strain (H77: AF009606), and four 1b strains (Con1: AJ238799, AB080299, AY045702, M58335), we found 14 amino acids variants unique to JFH-1 RdRP (57T, 130P, 131Q, 150A, 377R, 405I, 435V, 450S, 455N, 474M, 479H, 517K, 561F and 571S). We focused on five JFH-1-type amino acid substitutions (Q377R, A450S, S455N, R517K, and Y561F) that have been shown to increase the polymerase activity of 1b RdRP [13]. We introduced these JFH-1-type amino acid substitutions into J6CF RdRP, individually and in combination, to test their effects on polymerase activity. We also tested a J6CF RdRP variant with a R517K substitution because it was included in the J6/N3H+5BSLX-JFH1 replicon (see below), although it did not enhance the polymerase activity of 1b RdRP *in vitro* [13].

The RdRPs of HCV JFH-1 and J6CF and mutant variants were purified as indicated in the Materials and Methods and Fig. S1A. The polymerase activity of wild-type (wt) and mutant RdRPs was measured using a *de novo* transcription system (Fig. 1 and Fig. S1B). The activity of J6CF RdRP was 7.0±0.6% of that of JFH-1. Similar to results seen with 1b RdRP substitution variants, the single amino acid substitutions Q377R, A450S, S455N, R517K, and Y561F resulted in increased polymerase activity of J6CF RdRP (25.5±1.5, 27.7±1.0, 53.1±0.9, 16.9±3.5 and 16.7±2.5% of JFH-1 RdRP wt, respectively). However, combining double and triple amino acid substitutions did not demonstrate any additive or synergistic effects on the *in vitro* polymerase activity (Fig. 1).

JFH-1 RdRP variants with individual J6CF-type amino acid substitutions, including R377Q, S450A, N455S, K517R, and F561Y, were also examined *in vitro*. With the exception of N455S,

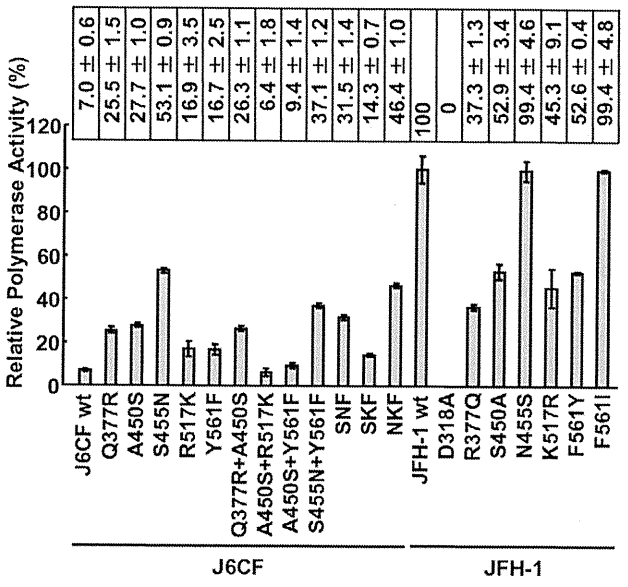

Figure 1. Relative HCV RNA polymerase activity of JFH-1 and J6CF wild-type and mutant RdRP. HCV RdRP activity was measured using the purified HCV RdRP (Fig. S1A) and the average RdRP activity and the standard deviation (error bar) relative to that of JFH-1 RdRP wt were calculated from three independent experiments (Representative gel images are shown in Fig. S1B). The relative activity values are presented above the graph. SNF, A450S+S455N+Y561F; SKF, A450S+R517K+Y561F; NKF, S455N+R517K+Y561F.
doi:10.1371/journal.ppat.1000885.g001

all other J6CF-type amino acid substitutions reduced the activity of JFH-1 RdRP, with levels ranging from 37.3 to 52.9% of the activity from wt JFH-1 RdRP (Fig. 1). The N455S variant maintained polymerase activity similar to that of JFH-1 wt. The JFH-1 D318A variant has a mutation in the active site of RdRP and showed no polymerase activity, confirming our *in vitro* transcription system.

JFH-1-type amino acid residues in the NS5B region restored the replication activity of the J6CF-based replicon

In order to test whether the JFH-1-type amino acids substitutions into the NS5B region of J6CF that enhanced polymerase activity *in vitro* enabled the replication of J6CF in cultured cells, we used the subgenomic J6CF replicon harboring the NS3 helicase region and 3′UTR of JFH-1 (J6/N3H+3′UTR-JFH1-Luc; Fig. 2A) as a reference construct. This replicon could replicate in cultured cells but exhibited less than 1% of the JFH-1 replication activity [12]. In order to test the effect of JFH-1 type amino acids on replication, we introduced the five substitutions that increased polymerase activity of J6CF RdRP *in vitro* (Q377R, A450S, S455N, R517K, and Y561F, see Fig. 2B) into the subgenomic replicon J6/N3H+3′UTR-JFH1-Luc and analyzed their effects on RNA replication. Among these JFH-1-type amino acids substitutions, Y561F was the most effective (23.2±3.5% of J6/N3H+N5BX-JFH1-Luc; Fig. 2C), while A450S, S455N, and R517K exhibited only a small effect on the replication activity (7.1±0.6%, 3.0±0.5%, and 5.5±1.0% of J6/N3H+N5BX-JFH1-Luc, respectively; Fig. 2C). The Q377R mutation demonstrated no effect on replication (Fig. 2C). We next tested the effects of Y561F in combination with each of the other substitutions. We found that A450S, S455N, and R517K mutations enhanced the replication activity of Y561F (59.1±6.1%, 43.9±6.6%, and 57.9±4.6% of J6/N3H+N5BX-JFH1-Luc, respectively; Fig. 2C). We also tested the effects of triple mutations and found that the replication activity of the SNF (A450S+S455N+Y561F) and SKF (A450S+R517K+Y561F) mutants demonstrated 86.8±6.0% and 112.2±7.9% replication activity of J6/N3H+N5BX-JFH1-Luc, respectively (Fig. 2C). In addition, we did not observe any significant differences between replicon activity of these mutants and that of J6/N3H+N5BX-JFH1-Luc. A combination of four mutations (SNKF; A450S+S455N+R517K+Y561F) resulted in similar activity as SKF (115.2±11.7% of J6/N3H+N5BX-JFH1-Luc; Fig. 2C). These results indicated that Y561F represented the most effective JFH-1-type mutation required for efficient replication, and that SKF and SNKF were sufficient to support replication activity equivalent to that of the replicon with the entire NS5B and 3′ UTR of JFH-1 (J6/N3H+N5BX-JFH1-Luc). The additive effects of the JFH-1-type NS5B substitutions on the replicon differed from results obtained with the *in vitro* polymerase activity assay.

Next, we examined whether these substitutions were sufficient for full-genome RNA replication and virus production. We used Huh-7.5.1 cells to assess virus production because Huh-7.5.1 is highly permissive for HCV propagation [9]. We found that J6/N3H+3′UTR-JFH1-Luc showed weak replication activity (Fig. 2C), and the core protein was not detectable in the culture medium of J6/N3H+3′UTR-JFH1-transfected cells (Fig. 3B). The constructs expressing A450S, S455N, or R517K substitution variants demonstrated only very low core levels in the supernatant, while the construct expressing the Y561F mutation underwent RNA replication and produced the core protein (Y561F; 15.5±3.0% of J6/N3H+N5BX-JFH1; Fig. 3B). Double mutants containing the Y561F mutation were found to produce greater amounts of core protein than the Y561F single mutant (A450S+Y561F, 57.4±3.3%; S455N+Y561F, 45.9±4.0%; and R517K+Y561F, 61.9±5.8% of J6/N3H+N5BX-JFH1; Fig. 3B). The triple mutant SNF (A450S+S455N+Y561F) produced more core protein than the double mutants (75.7±12.0% of J6/N3H+N5BX-JFH1; Fig. 3B). In addition, we observed that the core production from the SKF and SNKF mutant RNA-transfected cells was similar to the levels produced by J6/N3H+N5BX-JFH1 (111.5±8.8% and 119.0±5.1% of J6/N3H+N5BX-JFH1, respectively; Fig. 3B). We also measured infectivity of the supernatants from the mutant RNA-transfected cells at 72h after transfection (Fig. 3B). The levels of infectious titers correlated with the core levels among the tested constructs in this experiment. These results indicated that the SKF substitutions in the C-terminal region of NS5B were sufficient to elevate viral RNA replication and viral production.

Extra complementary sequence at the 5BSL3.2 kissing-loop interaction site of JFH-1 was essential for efficient replication

We observed a discrepancy between the *in vitro* RNA polymerase activity assay and the genome replication assay in the effects of the amino acid substitutions (Figs. 1 and 2C). Y561F was the most effective JFH-1-type amino acid substitution in the replication assay, while S455N was the most effective in the *in vitro* polymerase activity assay. As the kissing-loop interaction between 5BSL3.2 and 3′X are important for RNA replication and amino acid (aa) 561 encoding nucleotides are involved in the stem-loop 3.2 in the NS5B region (5BSL3.2) [7,16,22], we hypothesized that the cis-factor (genome structure) may also affect RNA replication in the cells. Thus, we constructed the subgenomic replicon J6/N3H+5BSLX-JFH1-Luc and the full genome construct J6/N3H+5BSLX-JFH1 that contained the NS3 helicase region and the 5BSL3-to-3′X region

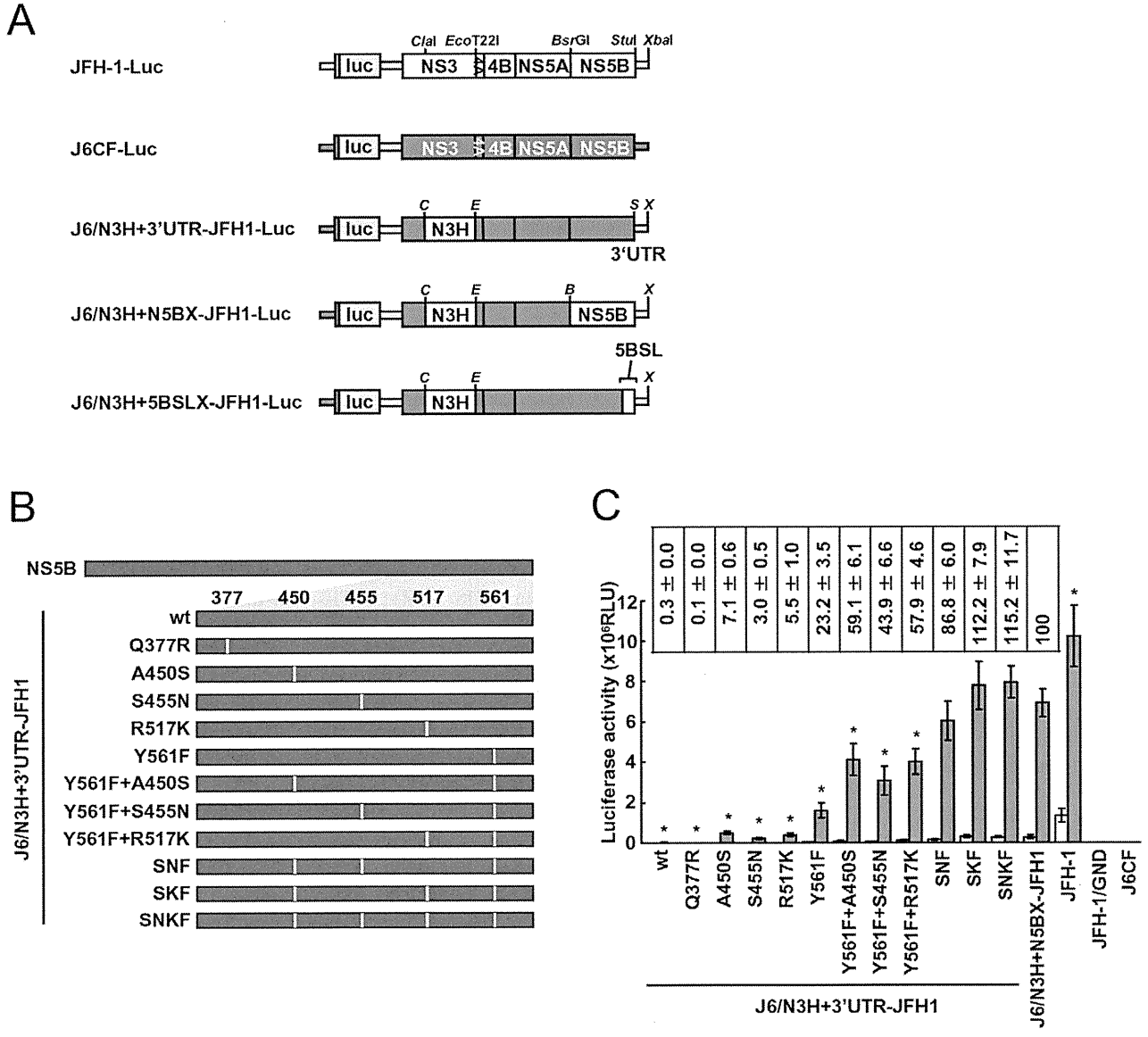

Figure 2. Luciferase activity of J6CF backbone replicons containing substitutions in the NS5B region. (A) Schematic structures of wt JFH-1 and J6CF constructs and the chimeric subgenomic replicons containing a J6CF backbone. The restriction enzyme recognition sites used for the construction of plasmids are indicated. *C, ClaI; E, Eco*T22I; *B, Bsr*GI; *S, StuI; X, XbaI*; wt, wild-type. (B) Schematic diagram of the mutations introduced into J6/N3H+3'UTR-JFH1-Luc and J6/N3H+3'UTR-JFH1. (C) Replication activity of J6CF-based replicons. Subgenomic RNA was synthesized *in vitro* from wild-type or chimeric replicon constructs. Transcribed subgenomic RNA (5 μg) was then electroporated into HuH-7 cells and the cells harvested at 4, 24, and 48 h after transfection. The harvested cells were lysed, and the luciferase activity in the cell lysates was measured. The assays were performed three times independently and the results expressed as luciferase activities (RLU). Each value was corrected for transfection efficiency as determined by measuring the luciferase activity 4 h after transfection. Data are presented as the mean ± standard deviation for luciferase activity at 24 h (white bars) and 48 h (gray bars) after transfection. Asterisks indicate significant differences relative to the replication activity of J6/N3H+N5BX-JFH1 ($p<0.05$) at 48 h and the values represent the relative values against J6/N3H+N5BX-JFH1 at 48 h after transfection. SNF, A450S+S455N+Y561F; SKF, A450S+R517K+Y561F; SNKF, A450S+ S455N+R517K+Y561F.
doi:10.1371/journal.ppat.1000885.g002

(nucleotide (nt) 9211 to 9678) of JFH-1 (Figs. 2A and 3A), and determined their replication activity and virus production level. As presented in Figure 4B, the J6/N3H+5BSLX-JFH1-Luc construct demonstrated similar replication activity to that of J6/N3H+N5BX-JFH1-Luc 48h post-transfection (92.9±7.5% of J6/N3H+N5BX-JFH1; Fig. 4B). Moreover, both J6/N3H+N5BX-JFH1 and J6/N3H+5BSLX-JFH1 released similar levels of core protein into the supernatant (Fig. 3B).

We next analyzed the effects of mutations in the J6/N3H+5BSLX-JFH1 construct. The 5BSL region of this construct contains three amino acid differences from J6CF (R517K, Y561F, and L571S). R517K and Y561F were important in the *in vitro* polymerase activity assay (Fig. 1). We did not assess aa 571 *in vitro* because it was deleted to purify HCV RdRP. The replication activities of J6/N3H+5BSLX-JFH1-Luc with K517R or F561Y were found to be 28±2.7% and 14±2.0% of J6/N3H+5BSLX-JFH1-Luc, respectively, confirming the importance of these JFH-1-type amino acids for replication (Fig. 4B). J6/N3H+5BSLX-JFH1-Luc with S571L revealed similar replicon activity as the J6/N3H+5BSLX-JFH1-Luc (108±7.8% of J6/N3H+5BSLX-JFH1

A

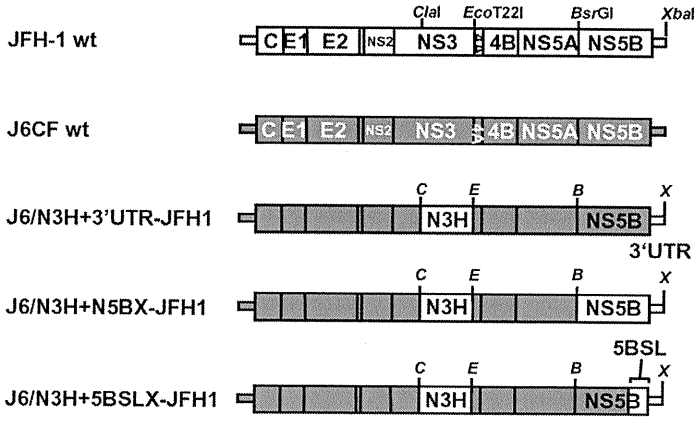

B

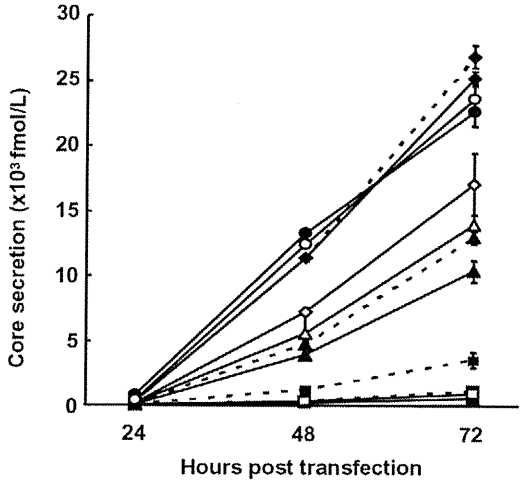

	Constructs	Core Secretion (%)	Infectivity (ffu/mL)
···◆···	SNKF	119.0 ± 5.1	$5.7x10^4$ ± $1.3x10^4$
—◆—	SKF	111.5 ± 8.8	$6.5x10^4$ ± $2.0x10^4$
—○—	J6/N3H+5BSLX-JFH1	104.7 ± 15.1	$5.8x10^4$ ± $4.7x10^3$
—●—	J6/N3H+N5BX-JFH1	100	$4.9x10^4$ ± $1.3x10^4$
—◇—	SNF	75.7 ± 12.0	$5.8x10^4$ ± $5.4x10^3$
—△—	R517K+Y561F	61.9 ± 5.8	$4.3x10^4$ ± $5.8x10^3$
···▲···	A450S+Y561F	57.4 ± 3.3	$2.6x10^4$ ± $6.9x10^3$
—▲—	S455N+Y561F	45.9 ± 4.0	$2.3x10^4$ ± $4.5x10^3$
···■···	Y561F	15.5 ± 3.0	$3.2x10^3$ ± $3.8x10^2$
—□—	R517K	4.2 ± 0.6	$7.0x10^1$ ± $1.0x10^1$
···□···	A450S	5.0 ± 0.1	$1.3x10^2$ ± $2.6x10^1$
—■—	S455N	2.7 ± 0.2	$1.4x10^2$ ± $3.1x10^1$
——	J6/N3H+3'UTR-JFH1	0.3 ± 0.1	$5.0x10^{-1}$ ± $0.0x10^0$

Figure 3. Analysis of transient replication of genomic chimeric HCV RNA. (A) The structure of full-length chimeric HCV RNA. Each chimeric full-length construct was prepared by the replacement of the indicated restricted fragments. The restriction enzyme recognition sites used for the plasmid constructions are indicated. *C, ClaI; E, Eco*T22I; *B, Bsr*GI; *S, StuI; X, XbaI*; wt, wild-type. (B) HCV core protein production in the culture medium from RNA-transfected cells. Transcribed wild-type or chimeric full-length HCV RNA (10 μg) was transfected into Huh-7.5.1 cells. Culture medium was harvested at 4, 24, 48, and 72 h after transfection. The amount of core protein in the harvested culture medium was measured using a HCV core chemiluminescence enzyme immunoassay (Lumipulse II HCV core assay). The assays were performed three times independently, and the data are presented as the mean ± standard deviation. Values in the right panel represent the relative core values against J6/N3H+N5BX-JFH1 at 72 h after transfection and infectious titers of the media from chimeric HCV RNA-transfected cells at 72h after transfection determined using Huh7.5.1 cells. SNF, A450S+S455N+Y561F; SKF, A450S+R517K+Y561F; SNKF, A450S+ S455N+R517K+Y561F.
doi:10.1371/journal.ppat.1000885.g003

wt; Fig. 4B). These results indicated the importance of 517K and 561F but not 571F in the 5BSL region of JFH-1 in efficient RNA replication. The codon encoding aa 561 possibly affects RNA structure, as it is located in the loop of stem-loop 3.2 in NS5B (5BSL3.2) and overlaps sequences important to the kissing-loop interaction with the stem loop 2 of the 3′X region (3′X SL2) [22]. Although we demonstrated that aa 561F was more effective than 561Y in RdRP activity *in vitro* (Fig. 1), it remains possible that the nucleotide mutation located at the codon of aa 561 affected the RNA structure and genome replication, as the replication activity of J6/N3H+3′UTR-JFH1-Luc with Y561F was the highest of all the clones with JFH-1 type single amino acids in the NS5B region (Fig. 2C). To investigate the effects of these mutations on RNA structure, we made mutants with nucleotide substitutions at the codon of aa 561 (Fig. 4F). The codon encoding aa 561 was UUU (Phe) for JFH-1 and UAU (Tyr) for J6CF. The third base of the codon overlaps with the kissing sequence [22]. In order to maintain the 5BSL3.2 stem loop structure and the kissing interaction between 5BSL3.2 and 3′X SL2, the third base should be U (nt 9349 of JFH-1). JFH-1 may exhibit additional interactions between 9348U of 5BSL3.2 and 9619A of 3′X SL2 to enhance kissing-loop interaction. To assess this hypothesis, we fixed the second base (9348) as U, and the first base (9347) was altered from U to A, G or C. The G and C substitutions were predicted to disrupt the important loop structure of 5BSL3.2 using Mfold and considered to affect replication activity. We next investigated the effects of U to A substitution (AUU, F561I) in an *in vitro* assay. F561I was introduced into JFH-1 RdRP and its RdRP activity was 99.4±4.8% of the wt, demonstrating that an F to I mutation did not affect polymerase activity (Fig. 1). We also examined the effects of the F561I mutation on RNA replication in the cells, and it revealed that it had similar replication activity as the wt,

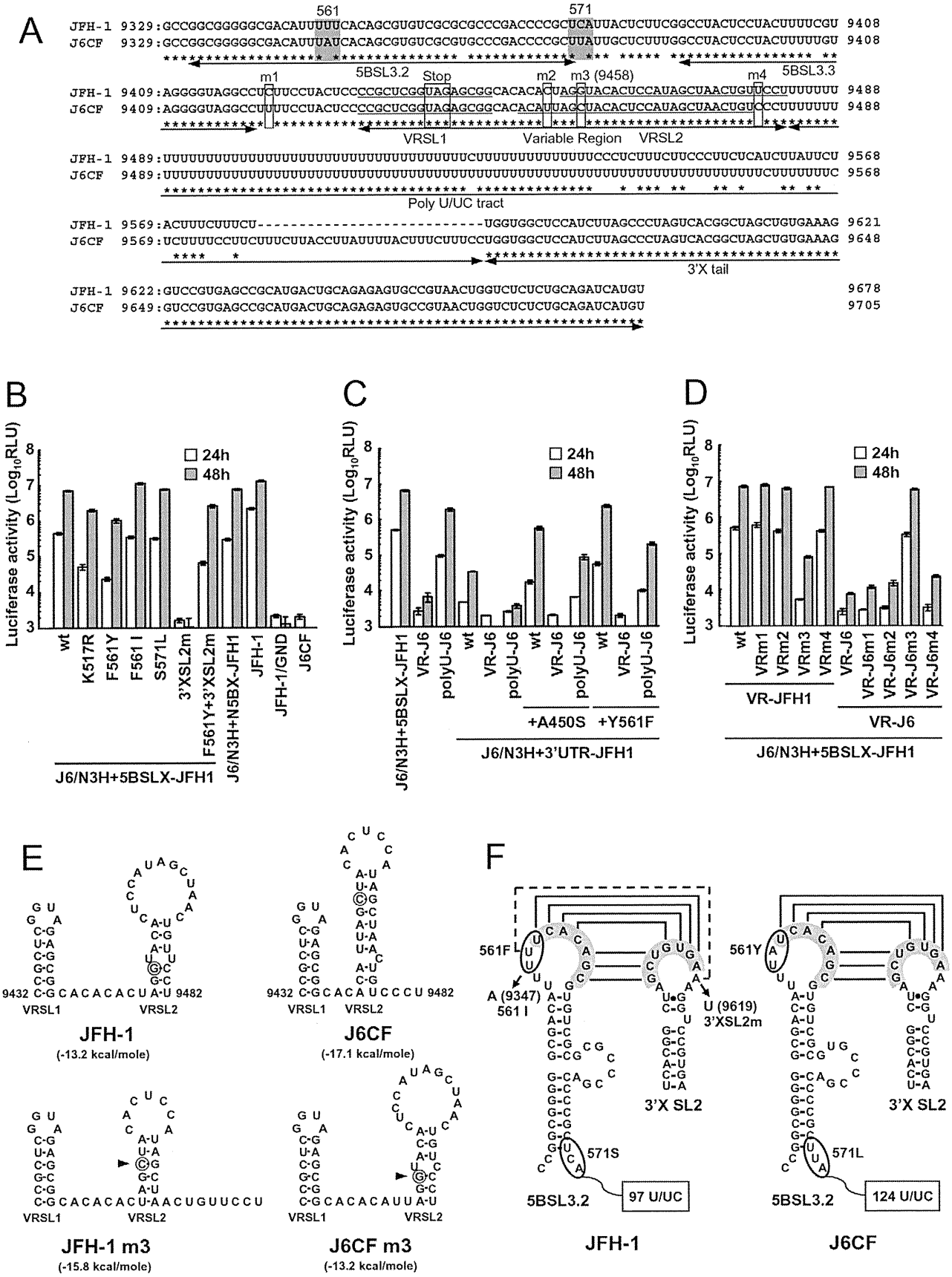
A
561
571
JFH-1 9329:GCCGGCGGGGGCGACAUUUUUCACAGCGUGUCGCGCGCCCGACCCCGCUCAUUACUCUUCGGCCUACUCCUACUUUUCGU 9408
J6CF 9329:GCCGGCGGGGGCGACAUUUAUCACAGCGUGUCGCGUGCCCGACCCCGCUUAUUGCUCUUUGGCCUACUCCUACUUUUUGU 9408
5BSL3.2
Stop
m1
m2
m3 (9458)
m4
5BSL3.3
JFH-1 9409:AGGGGUAGGCCUCUUCCUACUCCCCGCUCGGCUAGAGCGGCACACACUAGGUACACUCCAUAGCUAACUGUUCCUUUUUUU 9488
J6CF 9409:AGGGGUAGGCCUUUUCCUACUCCCCGCUCGGCUAGAGCGGCACACAUUAGCUACACUCCAUAGCUAACUGUCCCUUUUUUU 9488
VRSL1
Variable Region
VRSL2
JFH-1 9489:UUUUUUUUUUUUUUUUUUUUUUUUUUUUUUUUUUUUUUUUCUUUUUUUUUUUUUUUCCCUCUUUCUUCCCUUCUCAUCUUAUUCU 9568
J6CF 9489:UUUUUUUUUUUUUUUUUUUUUUUUUUUUUUUUUUUUUUUUUUUUUUUUUUUUUUUUUUUUUUUUUUUUUUUUUUUUUUUUUUC 9568
Poly U/UC tract
JFH-1 9569:ACUUUCUUUCU----------UGGUGGCUCCAUCUUAGCCCUAGUCACGGCUAGCUGUGAAAG 9621
J6CF 9569:UCUUUUCCUUCUUUCUUACCUUAUUUUACUUUCUUUCCUGGUGGCUCCAUCUUAGCCCUAGUCACGGCUAGCUGUGAAAG 9648
3'X tail
JFH-1 9622:GUCCGUGAGCCGCAUGACUGCAGAGAGUGCCGUAACUGGUCUCUCUGCAGAUCAUGU 9678
J6CF 9649:GUCCGUGAGCCGCAUGACUGCAGAGAGUGCCGUAACUGGUCUCUCUGCAGAUCAUGU 9705
B
Luciferase activity (Log10RLU)
24h
48h
wt
K517R
F561Y
F561 I
S571L
3'XSL2m
F561Y+3'XSL2m
J6/N3H+N5BX-JFH1
JFH-1
JFH-1/GND
J6CF
J6/N3H+5BSLX-JFH1
C
J6/N3H+5BSLX-JFH1
VR-J6
polyU-J6
+A450S
+Y561F
J6/N3H+3'UTR-JFH1
D
VRm1
VRm2
VRm3
VRm4
VR-J6m1
VR-J6m2
VR-J6m3
VR-J6m4
VR-JFH1
VR-J6
E
9432 C-G C A C A C A C U A-U 9482
VRSL1
VRSL2
JFH-1
(-13.2 kcal/mole)
9432 C-G C A C A U C C C U 9482
J6CF
(-17.1 kcal/mole)
C-G C A C A C A C U-A A C U G U U C C U
JFH-1 m3
(-15.8 kcal/mole)
C-G C A C A C A U U A-U
J6CF m3
(-13.2 kcal/mole)
F
561F
A (9347)
561 I
U (9619)
3'XSL2m
3'X SL2
571S
5BSL3.2
97 U/UC
JFH-1
561Y
571L
124 U/UC
J6CF

Figure 4. Replication activity of J6CF-based replicons containing variants or substitutions. (A) Comparison of the nucleotide sequence of 5BSL3.2 to 3′X of JFH-1 and J6CF. Boxes indicate nucleotide differences in VR and stop codon. Shaded boxes indicate non-synonymous variants in this region. 5BSL3.2, 5BSL3.3, Variable Region (VR), Poly U/UC tract, and 3′X tail are indicated by double-headed arrows in the figure. Stem-loop structures of VR (VRSL1 and VRSL2) are underlined. Asterisk; conserved nucleotides between JFH-1 and J6CF. (B, C, D) Replication activity of J6CF-based replicons. Five micrograms of *in vitro* synthesized RNA was electroporated into HuH-7 cells and the cells were harvested at 4, 24, and 48 h after transfection. The harvested cells were then lysed, and the luciferase activity in the cell lysates was measured. The assays were performed three times independently, and the results were expressed as luciferase activities (RLU). Data are presented as the mean ± standard deviation for luciferase activity at 24 h (white bars) and 48 h (gray bars) after transfection. (E) The predicted secondary structure of the VR. The RNA secondary structures of JFH-1, JFH-1 m3, J6CF, and J6CF m3 were predicated by Mfold. The stem-loop structure 1 (VRSL1) and 2 (VRSL2) are indicated. Nucleotide 9458 is circled and the mutated nucleotides are indicated by arrowheads. (F) Schematic structures of the 5BSL3.2 and X tail. The predicted stem loop structure of 5BSL3.2 and SL2 of 3′X of JFH-1 and J6CF strains are indicated. The sequences forming kissing interaction with 3′X SL2 [22] are shaded. Codons encoding aa 561 and 571 are circled and the mutated sequences are indicated. The reported kissing-loop interactions are indicated by the connecting lines. The predicted interaction of the JFH-1 strain is indicated by the dotted connecting line.
doi:10.1371/journal.ppat.1000885.g004

confirming that this mutation exhibited no effect on RNA replication in cultured cells (Fig. 4B). These results demonstrated that both Phe and Ile could be substituted at aa 561 and revealed the importance of the precise RNA structure of this region. Finally, we introduced an A to U mutation at nt 9619 in the 3′X SL2 that was complementary to the second base of the codon encoding 561F (9348) to alter the kissing-loop interaction (Fig. 4F; 3′XSL2m). We observed a significant reduction in 3′XSL2m replication activity (Fig. 4B; 3′XSL2m). However, when 3′XSL2m was combined with the F561Y mutation that was expected to recover the kissing-loop interaction, replicon activity was restored (Fig. 4B; F561Y+3′XSL2m). These results indicated that the extra complementary sequence at the kissing-loop interaction site of 5BSL3.2 was important for the efficient RNA replication of JFH-1. The extra complementary sequence may enhance the kissing loop interactions. We also tested the effect of the Y561F substitution on replicons of other genotypes, H77S (GT1a) and HCV-N (GT1b). While the Y561F substitution increased replication activity in both genotype 1 strains (Text S1 and Fig. S3), the Y561F effect on the genotype 1 strains was much smaller than its corresponding effect on J6CF.

A shorter poly U/UC sequence in the JFH-1 strain favored replication

We next compared the sequences of the poly U/UC tracts of the 3′UTRs of JFH-1 and J6CF. The poly U/UC tract of JFH-1 was 27 nucleotides shorter than that of J6CF (Figs. 4A and F). The polyU stretch of the pJ6CF plasmid that we used was six nucleotides shorter than that of the original J6CF sequence reported ([15], GenBank: AF177036). In order to analyze the effects of poly U/UC length on HCV replication, the poly U/UC region of J6/N3H+5BSLX-JFH1-Luc was replaced with that of J6CF and was designated as polyU-J6. The replicon activity of J6/N3H+5BSLX-JFH1-Luc with polyU-J6 was approximately four times lower than that of the J6/N3H+5BSLX-JFH1-Luc (Fig. 4C). This result showed that longer polyU/UC region lengths of J6CF were not favorable for efficient replication.

JFH-1 type structure of the variable region was advantageous for efficient replication

When we compared the VR sequences of the 3′UTRs of JFH-1 and J6CF, we found that four nucleotides are different between the VRs of JFH-1 and J6CF and that substitution of the VR from JFH-1 with that of J6CF of J6/N3H+5BSLX-JFH1 resulted in a 1000-fold decrease in replication activity (Fig. 4C, VR-J6). Mfold analysis of predicted RNA secondary structure of the VR in JFH-1 and J6CF suggests that there are two stem-loop structures in the VR. The first stem loop (VRSL1) structure is identical in JFH-1 and J6CF, but the loop of the second stem-loop (VRSL2) is larger in JFH-1 than in J6CF (Fig. 4E). Analysis of the effects of these nucleotide mutations on RNA structure revealed that only the third mutation (m3 at 9458 in Fig. 4A) is predicted to alter the structure of VRSL2 (Fig. 4E). The m3 G substitution into J6CF VR generated a predicted structure identical to that of JFH-1 VRSL2 resulting in identical VR structures (Fig. 4E). The m3 C substitution altered the structure of JFH-1 VR to the J6CF type (Fig. 4E). Substitutions of other nucleotides did not change the predicted structures (Data not shown). We then analyzed the effects of the mutations on replication activity. The m3 C substitution in JFH-1 VR was found to reduce replication activity 100-fold of the J6/N3H+5BSLX-JFH1-Luc (Fig. 4D; VRm3), whereas other substitutions (Fig. 4A; m1, m2 and m4) did not reduce replication activity at all (Fig. 4D; VRm1, VRm2 and VRm4). In contrast, the construct containing the J6CF VR with m3 G substitution completely restored replication activity (Fig. 4D; VR-J6m3). Other JFH-1 type nucleotide did not restore replication activity (Fig. 4D; VR-J6m1, VR-J6m2 and VR-J6m4). These results were in agreement with the stem-loop structure prediction of VR (Fig. 4E), demonstrating that the JFH-1 VR increased RNA replication. These results suggested the importance of VR secondary structure. Next, we tested if the effect of VR of JFH-1 was restricted to NS5B of JFH-1 or not. We constructed replicons with NS5B of J6CF and tested the effect on replication. The replication activities of the replicon with entire NS5B of J6CF (J6/N3H+3′UTR-JFH1), J6/N3H+3′UTR-JFH1 with A450S or Y561F (J6/N3H+3′UTR-JFH1+A450S, J6/N3H+3′UTR-JFH1+Y561F, respectively) were enhanced by the VR of JFH-1 (see polyU-J6 of each constructs in Fig. 4C) and not enhanced by the VR of J6CF (see VR-J6 of each constructs in Fig. 4C). These results indicated that the VR structure of JFH-1 was preferable for both JFH-1- and J6CF-derived NS5B and this effect was independent of the enhanced kissing-loop interaction (compare J6/N3H+3′UTR-JFH1 wt and A450S vs. Y561F in Fig. 4C).

Discussion

It has been demonstrated previously that HCV JFH-1, the only strain that replicates and produces virions efficiently in cell culture systems, expresses high replication activity without adaptive mutations [8]. We have previously reported that the N3H and N5BX regions of JFH-1 were able to rescue replication of the genotype 2a replicons [12]. The NS3 helicase and N5BX regions have been shown to be important to the virus production in HuH-7 cells. We have continued this line of experiment in the current study by focusing on RdRP activity and the genome structure in the 5BSL3.2 (CRE) to 3′X region. Following these aims, we were able to define the amino acids, nucleotides, and structural elements of JFH-1 required to confer replication competence and replication efficiency to the closely related J6CF.

In the present study, we identified five JFH-1-type amino acid residues in NS5B (Q377R, A450S, S455N, R517K, and Y561F) important for HCV replication by the *in vitro* polymerase activity assay and *in vivo* assays using replicons and full length HCV RNA. These amino acid residues are all in the thumb domain of HCV RdRP. All of these JFH-1-type substitutions increased the polymerase activity of J6CF RdRP. J6CF-type amino acids substitution into JFH-1 RdRP, including R377Q, S450A, K517R, and F561Y, reduced polymerase activity, while the N455S substitution demonstrated similar activity to the JFH-1 wt. The A450S and S455N substitutions resulted in the most significant enhancement of 1b [13] and J6CF RdRP (Fig. 1), respectively. aa 450 is located at the tip of the β-hairpin, while aa 455 is located close to the lower portions of the β-hairpin that may control the entry of the RNA template [13]. Both the β-hairpin (aa 450 to 455) and the β-strand (aa 560 to 565) of the thumb domain play an important role in RNA binding due to their extensive hydrogen-bonding network [23]. The β-hairpin has been shown to prevent the recruitment of the primer-template complex into the RNA-binding site to ensure accurate initiation from the 3′ end of the template [24,25]. A450S and S455N are thought to possibly affect J6CF RdRP structure by changing the spacing of the nucleic acid binding pocket occluded by the β-hairpin. As JFH-1 N455S did not decrease the polymerase activity of JFH-1, the thumb domain of JFH-1 may be optimized to control the position or movement of the β-hairpin. Simister *et al.* have recently reported that the higher *in vitro* polymerase activity of JFH-1 was due to a higher *de novo* initiation efficiency that may be due to a closed conformation of the JFH-1 polymerase [26]. Eight amino acid mutations in NS5B of JFH-1 are hypothesized to be responsible for the conformational differences in the NS5B sequences JFH-1 and the 2a consensus [26]. However, these amino acids did not overlap with the mutations that we identified to be important for replication. Taken together, these two studies suggested that the thumb structure surrounding the β-hairpin is important to RdRP activity [26]. We only tested six of 29 amino acid differences and other mutations are possibly important to RdRP activity. However, SKF and SNKF slightly increased replication activity compared to the replicon with entire NS5B of JFH-1 (Fig. 2C). These results suggest that there may be some JFH-1-type variants in NS5B region that inhibit the replication activity of JFH-1. The JFH-1 and J6CF 5BSL regions (Fig. S2) differ in three amino acids. The JFH-1-type substitution R517K and Y561F increased replication, while the variation at aa 571 did not affect replication. This means that there are no JFH-1 variants in 5BSL region that inhibit replication activity. However, some other mutations which were not tested outside of 5BSL region may inhibit replication. Taken together, we considered that is why the replicon with 5BSLX of JFH-1 had almost the same replication activity as the replicon with entire NS5B region of JFH-1.

After comparing the activating effects of A450S and S455N vs. R517K and Y561F in the *in vitro* polymerase, *in vivo* RNA replication and virus production assays, we hypothesized that amino acids 517 and 561 likely control HCV genome replication via interactions with additional host and viral factors, including the NS3 helicase and 3′UTR. A450S enhances polymerase activity alone, while R517K and Y561F enhance genome transcription and replication activity via additional factors. The aa 455 and 517 are known to be located at the surface of the polymerase, and these mutations may affect interactions with the proteins that play important roles in RNA replication.

The combination of A450S, R517K, and Y561F substitutions conferred replication activity to the replicon with J6CF RdRP. The results of the core production were in agreement with the results from the replicon assay and suggested that these amino acid mutations affected only RNA replication and did not affect the additional steps in the virus life cycle within the cells, such as virus particle assembly and virus secretion.

We did, however, observe a discrepancy between the effects of the mutations on *in vitro* RNA polymerase activity and *in vivo* RNA replication and virus production activities. The S455N mutation conferred the highest levels of activity on J6CF RdRP *in vitro*, while Y561F conferred the highest replication and virus production activities on J6/N3H+3′UTR-JFH1 in the cells. We did not observe any combination effects of the substitutions in the *in vitro* polymerase assays, while strong combination effects of the substitutions were observed on replication and core production *in vivo*. In addition, the combination of only three substitutions (SKF; A450S, R517K, and Y561F) was enough to increase HCV replication to levels similar to that of the construct harboring both the entire NS5B region and the 3′UTR of JFH-1. We did not observe any combination effects of the substitutions in the *in vitro* polymerase assays using 1b RdRP [13]. However, a discrepancy between polymerase activity *in vitro* and replication activity was also reported for GTP binding site mutants [27].

Discrepancies between the results from *in vitro* polymerase activity assays and *in vivo* replication assays may arise because of differences in the assay systems. In an *in vitro* polymerase assay, only enzymatic activity can be determined, while an *in vivo* assay of replication activity does not necessarily represent the only polymerase activity. Many viral and host factors may be involved in the RNA replication step in the cells. If a HCV replication assay using entirely reconstituted components were possible, we could compare the isolated effect of different polymerase variants on polymerase activity.

In addition to RdRP activity, host and viral factors, including *cis*-acting RNA structures in the 3′-genome must be considered in HCV replication in cells. In fact, we found a JFH-1-type nucleotide variant in NS5B region important to maintain the genome structure in the *in vivo* assay; this *cis*-acting factor could not have been identified using the *in vitro* polymerase assay. The SKF triple substitution contains the 561F variant that is important for enhanced kissing-loop interaction and high polymerase activity, suggesting that the effects of the SKF combination *in vivo* are rather due to the enhanced kissing-loop interaction.

We also analyzed the 5BSL3.2 and 3′XSL2 structures required for kissing-loop interactions, as aa 561 is in the loop domain of 5BSL3.2 and the activation effect of Y561F in the *in vivo* replicon assay was larger than in the *in vitro* polymerase assay. In order to test the effects of JFH-1-type variants of 5BSL3.2 on replication, we substituted the amino acids located downstream of the 5BSL3-to-3′X region (nt 9211 to 9678) from JFH-1 into the J6CF construct carrying the JFH-1-type NS3 helicase (J6/N3H+5BSLX-JFH1). The J6/N3H+5BSLX-JFH1 exhibited similar replication and virus production levels to J6/N3H+N5BX-JFH1. We initially focused on the amino acid differences between JFH-1 and J6CF in the region spanning between JFH-1 5BSL-to-3′X because this region was able to complement the entire JFH-1 NS5B-to-3′ X region. We identified three amino acid differences (517, 561, and 571) in the 5BSLX regions of JFH-1 and J6CF. We then introduced J6CF-type substitutions into the 5BSL3.2 region of JFH-1 RdRP. The J6CF-type substitution in JFH-1 5BSL3.2 region at positions 517 and 561, but not 571, resulted in a reduction in replication. These findings were consistent with the results of the *in vitro* polymerase assay. RNA polymerase activity *in vitro* was analyzed using the ΔC21-molecule (1–570) and JFH-1 RdRP that did not contain 571S demonstrated high levels of polymerase activity, indicating that 571S may not be important for

its high polymerase activity. The codon encoding aa 517 is located outside of the 5BSL3.2 region, suggesting that this mutation only affected polymerase activity. The codon encoding aa 561 and aa 571 are within the 5BSL3.2 region. The codon encoding aa 561 is located within the loop of the 5BSL3.2, while the codon encoding aa 571 is in the spacer region located between 5BSL3.2 and 5BSL3.3. The nucleotide mutations resulting the K517R and S571L aa substitutions were predicted to maintain 5BSL3.2 RNA secondary structures similar to that of JFH-1 using Mfold analysis [21].

Since there was the possibility that Y561F mutation affected both RdRP protein activity and genomic RNA structures, we tested the effect of nucleotide substitutions in the aa 561 codon on replication. The third nucleotide (9349U) contained within the codon encoding aa 561 is conserved among the different genotypes and essential for the kissing-loop interaction [16,22]. The second nucleotide (nt 9348) of JFH-1 is a U, while that of J6CF an A. The first nucleotide (nt 9347) of the codon should be either an A or a U, because these nucleotides are required to maintain the loop structure. Thus, a Phe (JFH-1), Tyr (J6CF and 1b), or Ile (9347A) may reside at position 561. As JFH-1 RdRP F561I retained identical activity levels to the wt (561F), hydrophobic amino acids appeared to be required in this position to maintain the high polymerase activity. Since the predicted secondary structures of 5BSL3.2 were identical for JFH-1 and J6CF, both Phe located at position 561 and the nucleotide sequence UUU in JFH-1 were essential for the high replication activity in cultured cells.

The conserved sequences of the kissing-loop interaction were UCACAGC (nt 9349–9355) in 5BSL3.2 and GCUGUGA (nt 9612–9618) in 3′X SL2. In the case of JFH-1, the nucleotide located at position 9348 was U and the nucleotide located at position 9619 was A, resulting in extended kissing-loop interaction sequence in JFH-1. When we introduced a mutation into the 3′X SL2 region (nt 9619) that was expected to abolish the extra base pair next to the interaction site, replication activity was significantly decreased. In addition, a combination of the F561Y and 3′X SL2m substitutions, expected to restore the extra base pair between nt 9348 and nt 9619, restored replication. Replication level of this double substitution was slightly lower than that of the wt constructs, possibly due to the preference for Phe at 561 over Tyr for genome replication. Mfold analysis also revealed that RNA secondary structure was not affected following the introduction of these substitutions. U at nucleotide position 9348 was previously identified in various HCV strains registered in GenBank [7]. Taken together, these findings suggested that the strong kissing-loop interaction of the JFH-1 genome supports efficient genome replication in HuH-7 cells. We also tested the effect of Y561F substitution in two other genotypes, H77S (GT1a) and HCV-N (GT1b). While the Y561F substitution increased replication activity in both genotype 1 strains, the Y561F effect on the genotype 1 strains was much smaller than its corresponding effect on J6CF. These results may indicate that the levels of Y561F effect for viral RNA replication are different among the genotypes. These results may also indicate that the Y561F substitution enhanced replication of strains with a substantial replication capacity. In case of J6CF, the Y561F effect was only observed with N3H region and VR of JFH-1 (Fig. 4C, compare VR-J6 and polyU-J6 of J6/N3H+3′UTR-JFH1+Y561F). This result suggested that the Y561F effect was difficult to detect with replication-incompetent clones or clones with weak replication, and also suggested that other mutations or regions are important to replicate genotype 1 replicon efficiently. Therefore, we need more efficient replicating clone of genotype 1 to determine the effect and importance of this mutation on genotype 1 strains.

We next analyzed the effects of 3′UTR structure on replication and demonstrated that the polyU/UC of JFH-1 was 27 nucleotides shorter than that of J6CF. The shorter polyU/UC and the RNA structure of the VR of JFH-1 appeared enhance efficient replication. When using the activated RdRP (SKF) and the optimal RNA structure of the 3′ genome together with the JFH-1 NS3 helicase, we found that J6CF, which did not replicate in cells, was successfully converted to a replicating virus. The VR sequence is generally not conserved, even among strains within the same genotype, and the effects of VR on HCV replication remain controversial [14,15,28]. Our data revealed that the VR of JFH-1 was more favorable than that of J6CF for replication. Substitution of the VR from JFH-1 to J6CF significantly reduced replication levels 1000-fold. This dramatic change in replication activity was likely due to alterations in the RNA structure with a mutation at nt 9458. The predicted RNA structure of the VR and replication activity of the constructs containing substitutions or mutations to the VR were completely correlated. It is therefore very likely that cellular and viral factors interact with the HCV genome in this region, and that the specific nucleotide sequence and higher structure of the VR may be essential for these interactions. There is a possibility of genetic interaction between the VR and NS5B region. These kinds of interaction may also affect on polymerase activity.

The length of the polyU/UC tract appeared to be flexible and even differed within the same genotype. Even though JFH-1 and J6CF shared an identical 3′X, the JFH-1 poly U/UC tract (nt 9483–nt 9579) was 27 U shorter than that of J6CF (nt 9483–nt 9606). Thus, we examined whether the polyU/UC tract could be exchanged between JFH-1 and J6CF. The J6/N3H+5BSLX-JFH1 variant that contained the J6CF polyU/UC exhibited a four-fold reduction in replication, demonstrating that the polyU/UC did indeed affect replication. Several published papers have investigated the affects of length on the polyU/UC region [14,15,16]. Several viral and cellular proteins have also been reported to interact with the polyU sequence [29,30,31,32,33,34,35,36]. The preferential length and nucleotide sequence of the polyU/UC may be determined by interaction with these factors.

In conclusion, we found that high RdRP activity, enhanced kissing-loop interaction between 5BSL3.2 and 3′X SL2, optimal VR structure and a shorter polyU/UC tract in JFH-1 contributed to the high levels of HCV RNA replication and virus production in cultured cells. As NS3 helicase region of JFH-1 is also important for replication and viral production of J6CF, the replication enhancing mechanism of NS3 helicase region should be analyzed.

Supporting Information

Figure S1 (A). Purified HCV J6CF and JFH-1 mutant RNA polymerases. HCV RdRp variants were purified as indicated in the Materials and Methods section. Five pmol of RdRp were applied on 10% SDS-PAGE and stained with Coomassie brilliant blue. The designations of HCV J6CF and JFH-1 wt and mutants are indicated above the PAGE. M; molecular weight marker (Takara), and the position is indicated on the left. (B). Representative PAGE of *in vitro* transcription of HCV J6CF and JFH-1 mutant RNA polymerases. *In vitro de novo* transcription was performed as indicated in the Materials and Method section. [^{32}P]-RNA products were applied on 6% PAGE containing 8 M urea. The autoradiography was analyzed by Typhoon trio plus image analyzer. The radio isotope count of 184 nt RNA product was measured and compared to that of JFH-1 RdRp wt in the same PAGE. The designations of HCV J6CF and JFH-1 wt and mutants are indicated above the PAGE. M; [^{32}P]-25 base DNA

ladder (Takara), and the position is indicated on the left. The position of 184 nt RNA product is indicated on the right.
Found at: doi:10.1371/journal.ppat.1000885.s001 (0.45 MB TIF)

Figure S2 Comparisons of the amino acid sequence of NS5B of JFH-1 and J6CF. The 5BSL region is indicated with a box.
Found at: doi:10.1371/journal.ppat.1000885.s002 (0.13 MB TIF)

Figure S3 Effect of Y561F substitution on replication activity of genotype 1 replicons. Replication activity of genotype 1a (H77S:(A)) and 1b (HCV-N:(B)) replicons. Subgenomic RNA was synthesized *in vitro* from wild-type or chimeric replicon constructs. Transcribed subgenomic RNA (5 μg) was then electroporated into HuH-7 cells and the cells serially harvested 4, 24, and 48 h after transfection. The harvested cells were lysed and the luciferase activity of the cell lysates was measured. The assays were performed three times independently, and the results expressed as luciferase activities (RLU). Luciferase activity is expressed as the change in RLU (n-fold) relative to the luciferase activity 4 h after transfection. Each value was corrected for transfection efficiency as determined by measuring the luciferase activity 4 h after transfection. Data are presented as the mean ± standard deviation for luciferase activity.
Found at: doi:10.1371/journal.ppat.1000885.s003 (0.08 MB TIF)

Table S1 Oligonucleotides used for construction.
Found at: doi:10.1371/journal.ppat.1000885.s004 (0.04 MB XLS)

Text S1 Supplementary materials and methods
Found at: doi:10.1371/journal.ppat.1000885.s005 (0.03 MB DOC)

Acknowledgments

We thank Y. Gao for her technical assistance. The pJ6CF plasmid was kindly provided by Jens Bukh. The pCVH77c plasmid was kindly provided by Robert H. Purcell. The pFKI389/neo/NS3-3′/wt plasmid was kindly provided by Ralf Bartenschlager. The pH77-S, pNNeo/3-5B, and pNNeo/3-5BΔGDD plasmids were kindly provided by Stanley M. Lemon.

Author Contributions

Conceived and designed the experiments: AM LW XT TS TK TW TT. Performed the experiments: AM LW XT. Analyzed the data: AM LW XT TS TK TW TT. Contributed reagents/materials/analysis tools: TD DA YT MM. Wrote the paper: AM LW TW TT.

References

1. Lemon S, Walker C, Alter M, Yi M (2007) Hepatitis C virus. In: Knipe D, Howley P, eds. Fields Virology 5 ed. PhiladelphiaPA: Lippincott-Raven Publishers. pp 1253–1304.
2. Wasley A, Alter MJ (2000) Epidemiology of hepatitis C: geographic differences and temporal trends. Semin Liver Dis 20: 1–16.
3. Grakoui A, Wychowski C, Lin C, Feinstone SM, Rice CM (1993) Expression and identification of hepatitis C virus polyprotein cleavage products. J Virol 67: 1385–1395.
4. Hijikata M, Mizushima H, Tanji Y, Komoda Y, Hirowatari Y, et al. (1993) Proteolytic processing and membrane association of putative nonstructural proteins of hepatitis C virus. Proc Natl Acad Sci U S A 90: 10773–10777.
5. Tsukiyama-Kohara K, Iizuka N, Kohara M, Nomoto A (1992) Internal ribosome entry site within hepatitis C virus RNA. J Virol 66: 1476–1483.
6. Tanaka T, Kato N, Cho MJ, Shimotohno K (1995) A novel sequence found at the 3′ terminus of hepatitis C virus genome. Biochem Biophys Res Commun 215: 744–749.
7. You S, Stump DD, Branch AD, Rice CM (2004) A cis-acting replication element in the sequence encoding the NS5B RNA-dependent RNA polymerase is required for hepatitis C virus RNA replication. J Virol 78: 1352–1366.
8. Wakita T, Pietschmann T, Kato T, Date T, Miyamoto M, et al. (2005) Production of infectious hepatitis C virus in tissue culture from a cloned viral genome. Nat Med 11: 791–796.
9. Zhong J, Gastaminza P, Cheng G, Kapadia S, Kato T, et al. (2005) Robust hepatitis C virus infection in vitro. Proc Natl Acad Sci U S A 102: 9294–9299.
10. Lindenbach BD, Evans MJ, Syder AJ, Wolk B, Tellinghuisen TL, et al. (2005) Complete replication of hepatitis C virus in cell culture. Science 309: 623–626.
11. Pietschmann T, Kaul A, Koutsoudakis G, Shavinskaya A, Kallis S, et al. (2006) Construction and characterization of infectious intragenotypic and intergenotypic hepatitis C virus chimeras. Proc Natl Acad Sci U S A 103: 7408–7413.
12. Murayama A, Date T, Morikawa K, Akazawa D, Miyamoto M, et al. (2007) The NS3 helicase and NS5B-to-3′X regions are important for efficient hepatitis C virus strain JFH-1 replication in Huh7 cells. J Virol 81: 8030–8040.
13. Weng L, Du J, Zhou J, Ding J, Wakita T, et al. (2009) Modification of hepatitis C virus 1b RNA polymerase to make a highly active JFH1-type polymerase by mutation of the thumb domain. Arch Virol 154: 765–773.
14. Friebe P, Bartenschlager R (2002) Genetic analysis of sequences in the 3′ nontranslated region of hepatitis C virus that are important for RNA replication. J Virol 76: 5326–5338.
15. Yanagi M, Purcell RH, Emerson SU, Bukh J (1999) Hepatitis C virus: an infectious molecular clone of a second major genotype (2a) and lack of viability of intertypic 1a and 2a chimeras. Virology 262: 250–263.
16. You S, Rice CM (2008) 3′ RNA elements in hepatitis C virus replication: kissing partners and long poly(U). J Virol 82: 184–195.
17. Nakabayashi H, Taketa K, Miyano K, Yamane T, Sato J (1982) Growth of human hepatoma cells lines with differentiated functions in chemically defined medium. Cancer Res 42: 3858–3863.
18. Kuiken C, Combet C, Bukh J, Shin IT, Deleage G, et al. (2006) A comprehensive system for consistent numbering of HCV sequences, proteins and epitopes. Hepatology 44: 1355–1361.
19. van den Hoff MJ, Moorman AF, Lamers WH (1992) Electroporation in 'intracellular' buffer increases cell survival. Nucleic Acids Res 20: 2902.
20. Kato T, Date T, Miyamoto M, Sugiyama M, Tanaka Y, et al. (2005) Detection of anti-hepatitis C virus effects of interferon and ribavirin by a sensitive replicon system. J Clin Microbiol 43: 5679–5684.
21. Zuker M (2003) Mfold web server for nucleic acid folding and hybridization prediction. Nucleic Acids Res 31: 3406–3415.
22. Friebe P, Boudet J, Simorre JP, Bartenschlager R (2005) Kissing-loop interaction in the 3′ end of the hepatitis C virus genome essential for RNA replication. J Virol 79: 380–392.
23. Leveque VJ, Johnson RB, Parsons S, Ren J, Xie C, et al. (2003) Identification of a C-terminal regulatory motif in hepatitis C virus RNA-dependent RNA polymerase: structural and biochemical analysis. J Virol 77: 9020–9028.
24. Zhong W, Ferrari E, Lesburg CA, Maag D, Ghosh SK, et al. (2000) Template/primer requirements and single nucleotide incorporation by hepatitis C virus nonstructural protein 5B polymerase. J Virol 74: 9134–9143.
25. Hong Z, Cameron CE, Walker MP, Castro C, Yao N, et al. (2001) A novel mechanism to ensure terminal initiation by hepatitis C virus NS5B polymerase. Virology 285: 6–11.
26. Simister P, Schmitt M, Geitmann M, Wicht O, Danielson UH, et al. (2009) Structural and functional analysis of hepatitis C virus strain JFH1 polymerase. J Virol.
27. Cai Z, Yi M, Zhang C, Luo G (2005) Mutagenesis analysis of the rGTP-specific binding site of hepatitis C virus RNA-dependent RNA polymerase. J Virol 79: 11607–11617.
28. Arumugaswami V, Remenyi R, Kanagavel V, Sue EY, Ngoc Ho T, et al. (2008) High-resolution functional profiling of hepatitis C virus genome. PLoS Pathog 4: e1000182. doi:10.1371/journal.ppat.1000182.
29. Kanai A, Tanabe K, Kohara M (1995) Poly(U) binding activity of hepatitis C virus NS3 protein, a putative RNA helicase. FEBS Lett 376: 221–224.
30. Luo G, Hamatake RK, Mathis DM, Racela J, Rigat KL, et al. (2000) De novo initiation of RNA synthesis by the RNA-dependent RNA polymerase (NS5B) of hepatitis C virus. J Virol 74: 851–863.
31. Huang L, Hwang J, Sharma SD, Hargittai MR, Chen Y, et al. (2005) Hepatitis C virus nonstructural protein 5A (NS5A) is an RNA-binding protein. J Biol Chem 280: 36417–36428.
32. Gontarek RR, Gutshall LL, Herold KM, Tsai J, Sathe GM, et al. (1999) hnRNP C and polypyrimidine tract-binding protein specifically interact with the pyrimidine-rich region within the 3′NTR of the HCV RNA genome. Nucleic Acids Res 27: 1457–1463.
33. Luo G (1999) Cellular proteins bind to the poly(U) tract of the 3′ untranslated region of hepatitis C virus RNA genome. Virology 256: 105–118.
34. Petrik J, Parker H, Alexander GJ (1999) Human hepatic glyceraldehyde-3-phosphate dehydrogenase binds to the poly(U) tract of the 3′ non-coding region of hepatitis C virus genomic RNA. J Gen Virol 80 (Pt12): 3109–3113.
35. Spangberg K, Wiklund L, Schwartz S (2001) Binding of the La autoantigen to the hepatitis C virus 3′ untranslated region protects the RNA from rapid degradation in vitro. J Gen Virol 82: 113–120.
36. Spangberg K, Wiklund L, Schwartz S (2000) HuR, a protein implicated in oncogene and growth factor mRNA decay, binds to the 3′ ends of hepatitis C virus RNA of both polarities. Virology 274: 378–390.

Biochemical and Biophysical Research Communications 395 (2010) 565–571

Contents lists available at ScienceDirect

Biochemical and Biophysical Research Communications

journal homepage: www.elsevier.com/locate/ybbrc

Biological properties of purified recombinant HCV particles with an epitope-tagged envelope

Hitoshi Takahashi [a,b], Daisuke Akazawa [a,b], Takanobu Kato [a], Tomoko Date [a], Masayuki Shirakura [a,b], Noriko Nakamura [b], Hidenori Mochizuki [b], Keiko Tanaka-Kaneko [c], Tetsutaro Sata [c], Yasuhito Tanaka [d], Masashi Mizokami [e], Tetsuro Suzuki [a], Takaji Wakita [a,*]

[a] Department of Virology II, National Institute of Infectious Diseases, Tokyo, Japan
[b] Toray Industries, Inc., Kanagawa, Japan
[c] Department of Pathology, National Institute of Infectious Diseases, Tokyo, Japan
[d] Department of Clinical Molecular Informative Medicine, Nagoya City University Graduate School of Medicine, Nagoya, Japan
[e] Research Center for Hepatitis & Immunology, Kohnodai Hospital, International Medical Center of Japan, Chiba, Japan

ARTICLE INFO

Article history:
Received 3 April 2010
Available online 23 April 2010

Keywords:
Hepatitis C virus
Envelope protein
Purification
Particle
Vaccine

ABSTRACT

To establish a simple system for purification of recombinant infectious hepatitis C virus (HCV) particles, we designed a chimeric J6/JFH-1 virus with a FLAG (FL)-epitope-tagged sequence at the N-terminal region of the E2 hypervariable region-1 (HVR1) gene (J6/JFH-1/1FL). We found that introduction of an adaptive mutation at the potential *N*-glycosylation site (E2N151K) leads to efficient production of the chimeric virus. This finding suggests the involvement of glycosylation at Asn within the envelope protein(s) in HCV morphogenesis.

To further analyze the biological properties of the purified recombinant HCV particles, we developed a strategy for large-scale production and purification of recombinant J6/JFH-1/1FL/E2N151K. Infectious particles were purified from the culture medium of J6/JFH-1/1FL/E2N151K-infected Huh-7 cells using anti-FLAG affinity chromatography in combination with ultrafiltration. Electron microscopy of the purified particles using negative staining showed spherical particle structures with a diameter of 40–60 nm and spike-like projections. Purified HCV particle-immunization induced both an anti-E2 and an anti-FLAG antibody response in immunized mice. This strategy may contribute to future detailed analysis of HCV particle structure and to HCV vaccine development.

1. Introduction

The hepatitis C virus (HCV) causes chronic hepatitis, liver cirrhosis and hepatocellular carcinoma [1]. HCV is a positive strand RNA virus belonging to the *Hepacivirus* genus in the Flaviviridae family. The HCV genome consists of about 9600 nucleotides and contains three regions: a 5′ non-coding region of 341 nucleotides containing the sequence for the IRES structure, a coding region of about 9000 nucleotides, which encodes about 10 viral proteins, and a 3′ non-coding region of about 200 nucleotides depending on the size of the poly-uridylate track within this region [2,3].

The main therapy for HCV is treatment with pegylated-interferon and rivabirin. However, these agents show little effect in patients that have a high titer of HCV RNA, genotype 1. Thus, it is necessary to develop new, more effective therapies and preventive treatments to counteract HCV infection. As yet, no preventive vaccine is available for HCV. A recombinant HCV vaccine based on the viral envelope protein E1/E2 has been reported that generated neutralizing antibodies (nAb) in animals [4]. These nAbs were capable of limiting HCV pseudoparticles (HCVpp) and HCV cell culture (HCVcc) infection.

Recently, a genotype 2a strain of HCV named JFH-1 was discovered. This strain can efficiently replicate in the Huh-7 cell line [5], and an *in vitro* culture system of infectious HCV has also been successfully developed using the JFH-1 genome [6–8]. The JFH-1 viral production system is expected to become a powerful tool for HCV vaccine development. In this study, we developed a simple strategy for purification of recombinant HCV particles from the media of infected Huh-7 cells for structural analysis and for vaccine development using the JFH-1 genome.

2. Materials and methods

2.1. Plasmids

Plasmid pJ6/JFH-1 was generated from pJFH-1 by replacement of the 5′ untranslated region with the p7 region of J6 [9]. The

* Corresponding author. Address: Department of Virology II, National Institute of Infectious Diseases, 1-23-1 Toyama, Shinjuku, Tokyo 162-8640, Japan. Fax: +81 3 5285 1161.
E-mail address: wakita@nih.go.jp (T. Wakita).

0006-291X/$ - see front matter © 2010 Elsevier Inc. All rights reserved.
doi:10.1016/j.bbrc.2010.04.081

plasmids pJ6/JFH-1/1FL and pJ6/JFH-1/3FL were constructed by introduction of a single (DYKDDDDKGGG) or triple (DYKDHDG-DYKDHDIDYKDDDDKGGG) FLAG-tag sequence, respectively, into pJ6/JFH-1, which replaced part of the E2 HVR1 (amino acids 394–400) region. These two plasmids were then modified by introduction of a Lys residue to replace the Asn at amino acid position 151 of the E2 sequence, creating pJ6/JFH-1/1FL/E2N151K and pJ6/JFH-1/3FL/E2N151K, respectively.

The J6E2 gene (codons 1490–2500) was generated by PCR amplification from pJ6CF. The sense and antisense primers used were: 5′-CACAAGCTTCGCACCCATACTGTTGGGG-3′ and 5′-ACAGGATCCCAT-CGGACGATGTATTTTGTG-3′, respectively. For cloning purposes, HindIII or BamHI sites (underlined) were added to the primers. The amplified DNA was digested and inserted into p3XFLAG-CMV-13 (SIGMA, Saint Louis, MO).

The plasmid CDM-J6E2Fc encodes the J6E2 sequence downstream of the preprotrypsin leader sequence. pCDM-J6E2Fc was digested with SacI and BamHI, and the DNA fragment containing the preprotrypsin leader and J6E2 sequence was inserted into pCD4Rg (a kind gift from Dr. Brian Seed, Harvard Medical School) from which the SacI–BamHI fragment containing the CD4 gene was removed. This ligation resulted in the creation of a plasmid encoding a fusion gene of E2 and human IgG1-Fc.

2.2. Cell culture

The human hepatoma cell line, Huh-7, was maintained in DMEM supplemented with 10% FBS at 37 °C in a 5% CO_2 incubator.

2.3. In vitro synthesis of HCV RNA and RNA transfection of Huh cells

HCV RNA was synthesized from the plasmids described above *in vitro* using a MEGAscript T7 kit (Ambion, Austin, TX). Synthesized HCV RNA was then electroporated into cells as previously described [10]. The transfected cells were transferred onto 100-mm culture dishes containing culture medium.

2.4. Quantification of HCV core protein and RNA

The HCV core protein in cell culture supernatants or in purified HCV samples was quantified by enzyme immunoassay using a HCV core ELISA kit (Ortho Clinical Diagnostics). HCV RNA in purified HCV samples was quantified by RTD-PCR as previously described [11].

2.5. Deglycosylation with PNGase F

For deglycosylation reactions, the Enzymatic In-Solution N-Deglycosylation kit (Sigma) was used according to the manufacturer's instructions. Briefly, lysates of passaged cells were incubated for 10 min at 100 °C in denaturation buffer and then in the presence of PNGase F enzyme for 1 h at 37 °C. These samples were analyzed by Western blotting as described below using anti-FLAG (SIGMA) and anti-GAPDH (CHEMICON, Temecula, CA) antibodies.

2.6. Sequence analysis

The cDNAs of the HCV genome were synthesized from total RNA isolated from HCV RNA-transfected cells [5]. These cDNA were subsequently amplified using DNA polymerase (*TaKaRa LA Taq*, Takara, Shiga, Japan). The sequence of the amplified DNA was determined by the 3130 Genetic Analyzer (Applied Biosystems, Foster city, CA).

2.7. Purification of recombinant HCV particles

Culture supernatants from Huh-7 cells transfected with FLAG-tagged HCV RNA were harvested. The medium was concentrated by ultrafiltration using the pellicon-2 300 system (Millipore, Bedford, MA) and was subjected to affinity chromatography using an Anti-FLAG M2 affinity gel (Sigma). Virus particles were eluted using the 3×FLAG Peptide (Sigma) and were concentrated by ultracentrifugation for 2 h at 50,000 rpm at 4 °C.

2.8. Determination of the viral infectious titer

The infectious titer was determined by the method as previously described and was expressed as the number of focus-forming units per milliliter (FFU/mL) [6].

2.9. Western blotting

The purified HCV sample was lysed using a buffer containing 0.1 M Tris–HCl (pH 6.8), 4% SDS, 1.2% 2-mercaptoethanol, 20% glycerol, and Bromophenol blue. SDS–PAGE and immunoblotting were performed as previously described [6]. Antibodies used for immunoblotting were: anti-HCV core (clone 2H9) [6], anti-E1 (B7567) [6], and anti-E2 (clone 8D10-3, unpublished).

2.10. Electron microscopy

Concentrated, purified HCV particles were allowed to settle on carbon-coated copper grids and were stained with 4% uranylacetate. The grids were examined in a transmission electron microscope (H-7650, Hitachi, Tokyo, Japan) and were photographed at an instrumental magnification of 50,000×.

2.11. Sucrose density gradient analysis

The purified HCV sample containing 266 fmol of the HCV core was layered on a stepwise sucrose gradient (10–60%, wt/vol) and was centrifuged for 16 h in an SW41 rotor (Beckman Coulter, Fullerton, CA) at 35,000 rpm at 4 °C. After centrifugation, 12 fractions were harvested from the bottoms of the tubes. For each fraction, the core protein concentration was determined using an immunoassay. The HCV RNA titer was determined using RTD-PCR. The infectious titer was determined using an immunofluorescence assay as described above.

2.12. HCV particle-immunization

The purified HCV particles described above were inactivated by UV-irradiation, and 2 pmol of the HCV core protein of the particles were intraperitoneally injected into 4 week old BALB/c female mice ($n = 3$). Immunization was repeated four times at 2-week intervals (0, 2, 4 and 6 weeks). The Sigma Adjuvant System (Sigma), composed of monophosphoryl lipid A and trehalose dicorynomycolate, was used as an adjuvant. Saline alone was injected into control mice. Sera were collected at 1, 3, 5 and 7 weeks after immunization.

2.13. EIA for measurement of anti-E2 and anti-FLAG antibody responses

Recombinant J6E2/Fc or the FLAG peptide antigen (Sigma) was bound to microtiter plates (Nunc, Rochester, NY, USA) overnight at 4 °C, at a concentration of 50 ng per well. Recombinant J6E2/Fc was produced from COS-1 cells transfected with the CDM-J6E2Fc plasmid, which encodes the J6CF-E2 region (aa 384–720) fused with the Fc region of human IgG. The plates were blocked with Blocking One solution (Nacalai Tesque, Kyoto, Japan) and were washed with PBS containing 0.05% Tween 20 (washing buffer). Serum samples were diluted in washing buffer and were transferred to the blocked, antigen coated plates. After a 1.5-h incubation,

the plates were washed and bound antibody was detected using an HRP-conjugated anti-mouse antibody (GE healthcare, Buckinghamshire, England) and 3,3′,5,5′-tetramethylbenzidine (TMBZ) as a substrate (Sumitomo Bakelite, Tokyo, Japan).

3. Results

3.1. Production of recombinant HCV with an epitope-tagged envelope

To facilitate purification of recombinant HCV particles secreted into the culture medium of transfected cells, we constructed recombinant HCV with a FLAG-epitope-tagged envelope, which could then be purified by affinity chromatography using an anti-FLAG-agarose column. The FLAG-tagged HCV genome J6/JFH-1/3FL with the J6CF structural region was constructed by introducing a triple FLAG-tag sequence into the HVR1 of E2 (Fig. 1A). This region was selected for epitope-tag insertion because we predicted that this region would lie on the outside of the virus particles and would be tolerant to amino acid changes. Recombinant HCV particles were produced following transfection of Huh-7 cells with viral RNA, and were secreted into the culture medium.

RNA-transfected cells were passaged every 4 or 5 days. The level of the HCV core protein in the culture supernatant was measured over a period of 70 days (Fig. 1B). In contrast to the gradually increasing level of the core protein in J6/JFH-1 cells over time, the level of the core protein in the supernatants of the J6/JFH-1/3FL RNA-transfected cells decreased over the first 3 weeks post-transfection. Subsequently, the level began to increase and this level became equal to that of the wild-type J6/JFH-1 RNA-transfected cells 35 days post-transfection. This result suggested that after the first 35 days of culture, some mutations were introduced into the HCV genome that conferred efficient virus production during genome replication and/or that the transfected cells were altered in some way that was more favorable for viral production.

3.2. An N151K mutation facilitates the production of FLAG-tagged HCV

To determine if any adaptive mutations had arisen in the viral genome, we sequenced the full length of the HCV genome on days 8 and 35 post-J6/JFH-1/3FL RNA transfection. On day 8 post-transfection, no non-synonymous mutations were detected. However, on day 35, we found a single amino acid mutation at a potential

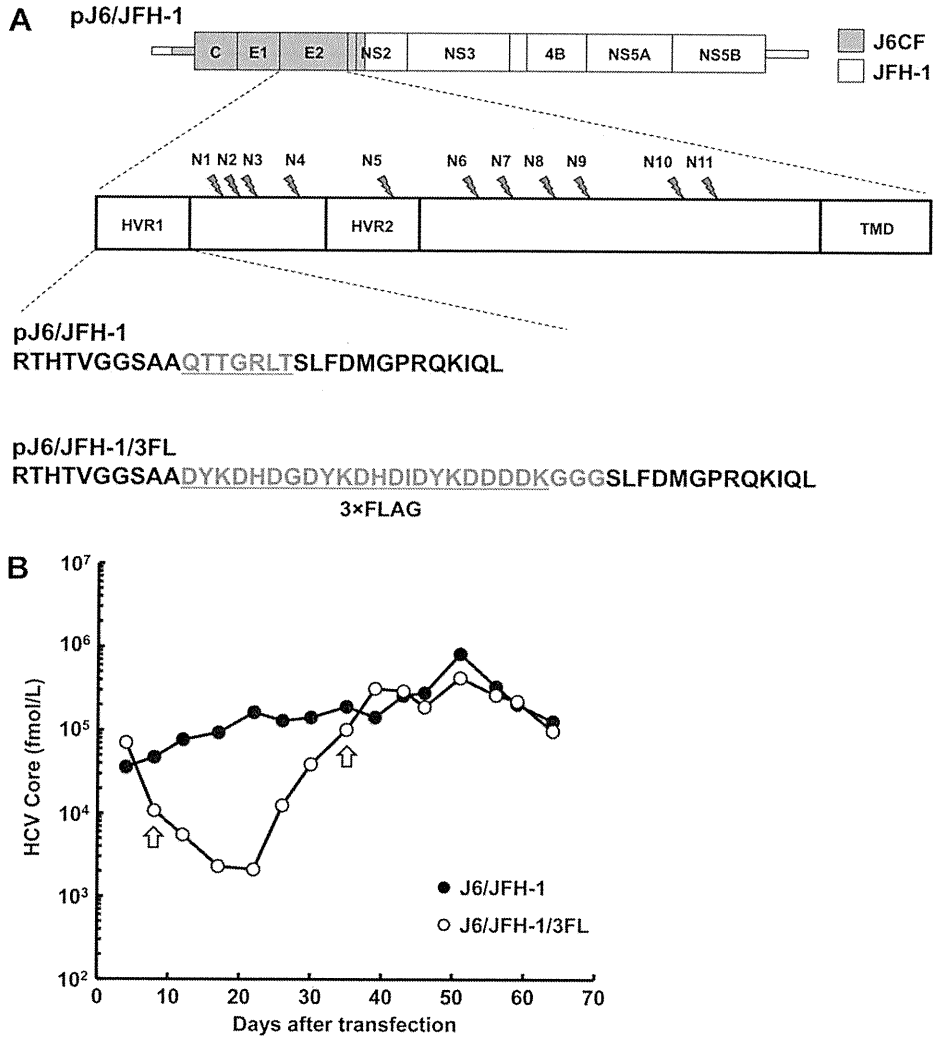

Fig. 1. Time course of HCV core protein secretion in recombinant HCV RNA-transfected cells. (A) Organization of the recombinant HCV construct pJ6/JFH-1/3FL. Open reading frames (thick boxes) are flanked by 5′- and 3′-UTRs (thin boxes). Gray, J6CF; white, JFH-1; HVR, hyper variable region; TMD, transmembrane domain. *N*-Glycosylation sites are indicated by pointers and are numbered N1–N11. The region of pJ6/JFH-1 that is replaced by the 3×FLAG sequence to generate pJ6/JFH-1/3FL is indicated at bottom. (B) HCV core protein secretion into the culture medium after HCV RNA transfection of Huh-7 cells. The HCV core protein was analyzed using an ELISA. Arrows indicate the times at which the J6/JFH-1/3FL HCV genome transfected into HCV RNA-transfected cells was sequenced.

N-glycosylation site of the E2 protein (Fig. 2A) in which asparagine at amino acid position 151 in the E2 protein was changed to lysine (E2N151K). Interestingly, this mutation was identical to that described by Delgrange et al. [12] as a mutation that was important for efficient production of HCV JFH-1. We performed Western blot analysis of cell lysates of transfected cells of different passages, using the anti-FLAG antibody as a probe for E2, to confirm that the N151K mutation abolishes one specific *N*-glycosylation. Indeed, the size of the FLAG-E2 protein was smaller on days 30 and 43 compared to that on day 4 (Fig. 2B). In contrast, the size of FLAG-E2 proteins that were deglycosylated using PNGase F was similar for all of the tested samples (Fig. 2B). This result suggested that the E2N151K mutation abolished *N*-glycosylation at this residue.

To investigate if the E2N151K mutation enhances production of FLAG-tagged HCV, we introduced the E2N151K mutation into the J6/JFH-1/3FL genome (J6/JFH-1/3FL/E2N151K). J6/JFH-1/3FL/E2N151K RNA-transfected cells were then passaged every 4 or 5 days and the level of the HCV core protein in the culture supernatant was measured over a period of 16 days (Fig. 2C). The result clearly showed that the E2N151K mutation contributes to efficient production of FLAG-tagged HCV particles.

We further analyzed the effect of the E2N151K mutation on specific viral infectivity (Table 1). The culture supernatant on day 3 post-transfection of recombinant viral RNA was therefore concentrated by ultrafiltration and tested in an infectious assay. The recombinant virus with the E2N151K mutation exhibited higher specific infectivity than the virus without this mutation. These data suggest that efficient production of infectious particles is impaired by the introduction of a FLAG-tag into the E2 protein but that this deficiency could be compensated for by the introduction of the E2N151K mutation which modifies an *N*-glycosylation site.

3.3. Purification of FLAG-tagged HCV

To purify FLAG-tagged HCV particles, we used a viral construct with a single FLAG-tag, J6/JFH-1/1FL/E2N151K (Fig. 1A), which as efficient in virus production as J6/JFH-1/3FL/E2N151K (data not shown). A total of 10 L of the culture supernatant of Huh-7 cells infected with J6/JFH-1/1FL/E2N151K was collected. This culture medium was concentrated to 300 mL by ultrafiltration and was then subjected to affinity chromatography using an anti-FLAG-agarose column. Bound virus particles were eluted using 10 mL of a

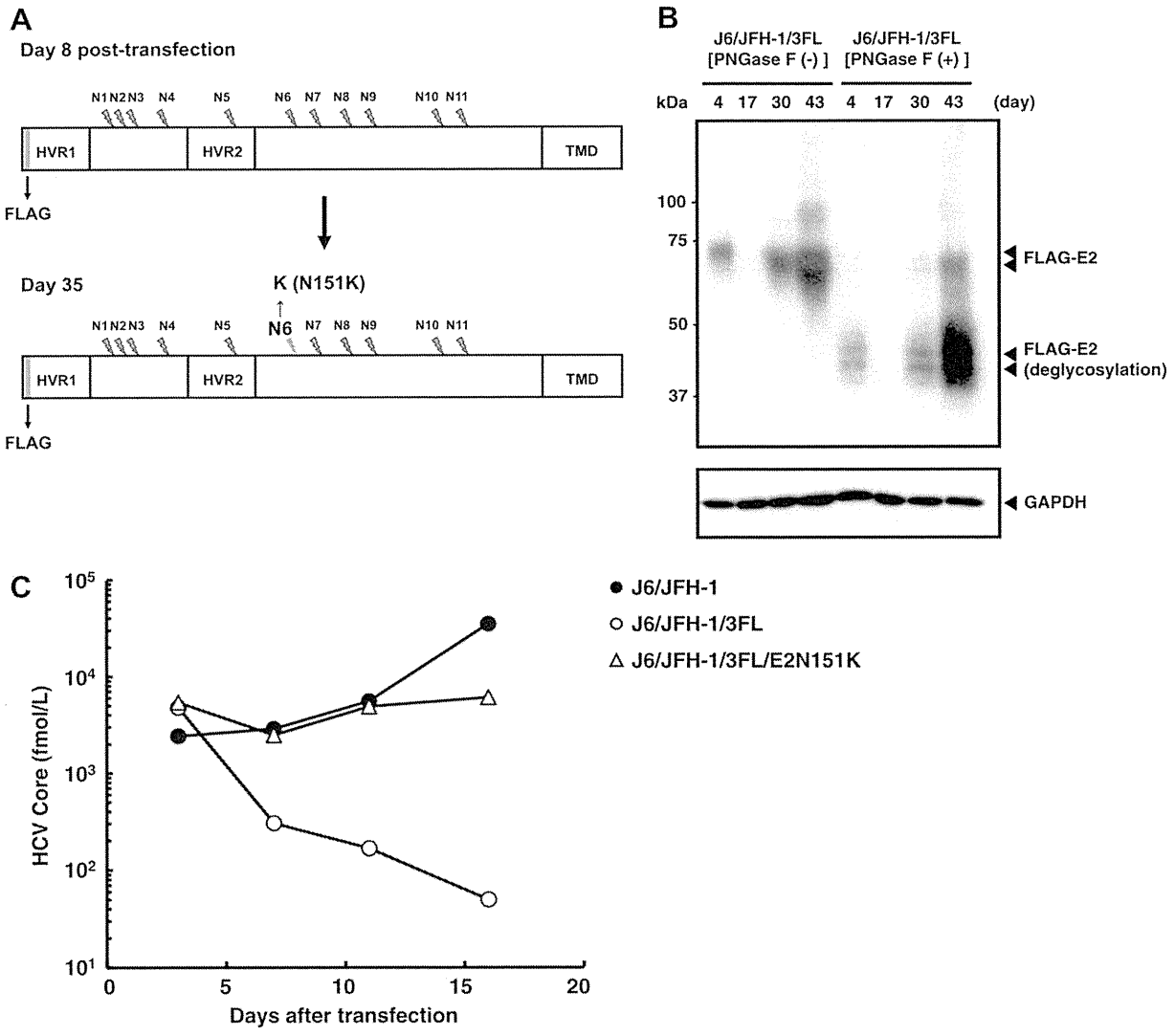

Fig. 2. Characterization of the recombinant HCV genome with an introduced N151K mutation. (A) Schematic diagram of the sequence of the E2 in the J6/JFH-1/3FL HCV RNA-transfected cells on day 8 and day 35 post-transfection. N151K replaces an Asn residue with a Lys residue at the N6 glycosylation site of E2. (B) Western blot analysis of the FLAG-E2 protein in lysates of cells transfected with J6/JFH-1/3FL RNA. Arrowheads indicate intact, and deglycosylated (PNGase F (+)), FLAG-E2 protein (upper panel) and control GAPDH protein (lower panel). (C) HCV core protein secretion into the culture medium following transfection of Huh-7 cells with HCV RNA with or without an introduced N151K mutation.

Table 1
Infectivity of recombinant viruses with or without N151K mutation.

Recombinant virus	Infectious titer ($\times 10^2$ FFU/mL)	HCV core protein ($\times 10^2$ fmol/mL)	Specific infectivity (FFU/HCV core)
J6/JFH-1/3FL	<1.7	1.6	<1.1
J6/JFH-1/3FL/E2N151K	8.3	2.0	4.2

FLAG peptide solution. Finally, the purified HCV particles were concentrated by ultracentrifugation.

The HCV yield and the amount of total protein after each purification step are summarized in Table 2. This purification process resulted in a 5000-fold concentration of the culture supernatant. The recovery of the HCV core protein in the final purified virus preparation was approximately 5%, and the virus purity was increased about 9000-fold compared to its purity in the initial culture medium. Specific infectivity was increased about 4-fold after the final step.

HCV structural proteins in the purified virus sample were examined by Western blotting (Fig. 3A). Core, E1 and E2 proteins were all detected in the purified virus preparation. Interestingly, incorporation of the E2 protein into the purified virus appeared to increase compared to incorporation of the core and E1 proteins. However, this higher apparent incorporation of FLAG-E2, may reflect the presence of free, non-virus incorporated FLAG-E2 proteins that co-purified with the FLAG-tagged virus. We further analyzed the virus particles in the purified preparation by electron microscopy (Fig. 3B–D). Substantial debris was found in the culture

Table 2
HCV yield and properties of purified recombinant HCV after each purification step.

Purification step	Volume (mL)	HCV core protein ($\times 10^2$ fmol/mL)	HCV RNA ($\times 10^7$ copies/mL)	Total protein (μg/mL)	Recovery[a] (%)	Purity[b]	Infectivity ($\times 10^2$ FFU/mL)	Specific infectivity (FFU/HCV core)
Culture supernatant	10,000	1.4	3.5	877	100	1	25	18
Concentrate (after Ultrafiltration)	300	45	57	19,597	96	0.73	743	17
Affinity purification (after Elution)	10	98	324	171	7	469	4240	43
Concentrate (after Ultracentrifugation)	0.2	1440	3220	84	5	9546	94,600	66

[a] Recovery of HCV core protein.
[b] The degree of virus purity was calculated by HCV RNA contents per μg total proteins.

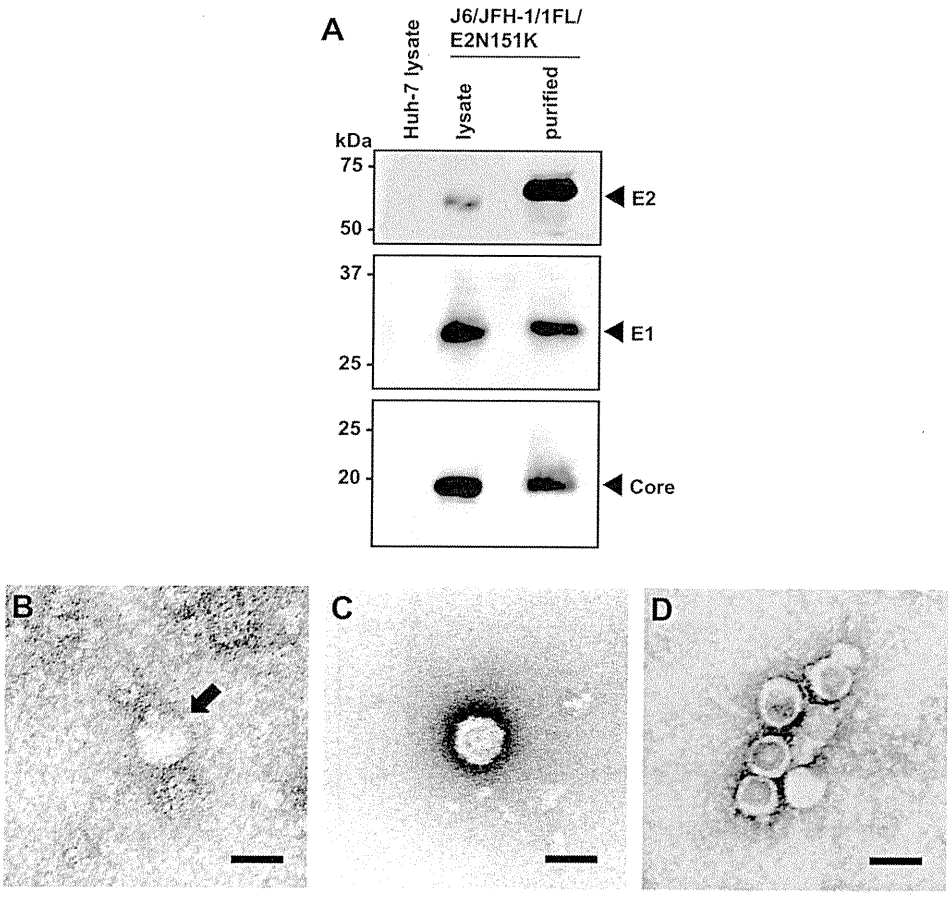

Fig. 3. Analysis of purified HCV particles. (A) Western blot analysis of viral proteins in lysates of, and in HCV particles purified from, whole-cell extracts of Huh-7 cells transfected with J6/JFH-1/1FL N151K RNA. Lysates of non-transfected cells were also analyzed. The arrowheads indicate the positions of the HCV core, E1 and E2 proteins. Marker proteins are shown at left. (B–D) Electron micrographs using negative staining of: (B) An HCV particle from culture media (indicated by an arrow.), (C) A purified HCV particle and (D) Purified HCV particles aggregated by an anti-FLAG antibody. Scale bar, 50 nm.

supernatant concentrated by ultrafiltration, which made it difficult to identify virus particles (Fig. 3B). In contrast, spherical particle structures of 40–60 nm could be clearly observed in the purified samples (Fig. 3C and D). Furthermore, the purified FLAG-tagged HCV particles were aggregated by the anti-FLAG antibody (Fig. 3D). The size and morphology of the FLAG-tagged particles were similar to each other but with slight deviations. The combined data suggest that the FLAG-tagged HCV particles can be purified by affinity chromatography using anti-FLAG-agarose.

3.4. Physical properties of purified FLAG-tagged HCV

We next further analyzed the properties of the purified FLAG-tagged HCV particles. The total number of proteins in the purified viral sample, as judged by SDS–PAGE and silver staining analysis, was much lower than that in the original culture medium (Fig. 4A). We confirmed by mass spectrometry analysis that these extra protein bands in the purified preparation were not viral proteins but were host proteins that bound to the FLAG-agarose (data not shown).

We further analyzed the purified FLAG-tagged HCV particles using a sucrose density gradient (Fig 4B). Purified virus was layered on top of a preformed continuous 10–60% sucrose gradient and was then centrifuged. Twelve fractions were collected and the HCV core protein, RNA and viral infectivity were determined for each fraction. The HCV particles migrated at a density between 1.13 and 1.16 g sucrose/mL. The density at which the peak of the HCV core protein was observed was almost identical to the density at which the HCV RNA and infectivity were detected.

3.5. Immunogenicity of purified HCV particles

To examine the immunogenicity of the FLAG-tagged HCV particles, they were injected into BALB/c mice and the sera of these mice were then analyzed for reactivity with recombinant J6E2/Fc or the FLAG peptide using an ELISA. The HCV particles were inactivated by UV-irradiation prior to injection using the Sigma Adjuvant System as an adjuvant. Both anti-E2 and anti-FLAG antibodies were induced in mice sera after four immunizations (Fig. 4C). These results suggested that the envelope proteins of the FLAG-tagged HCV

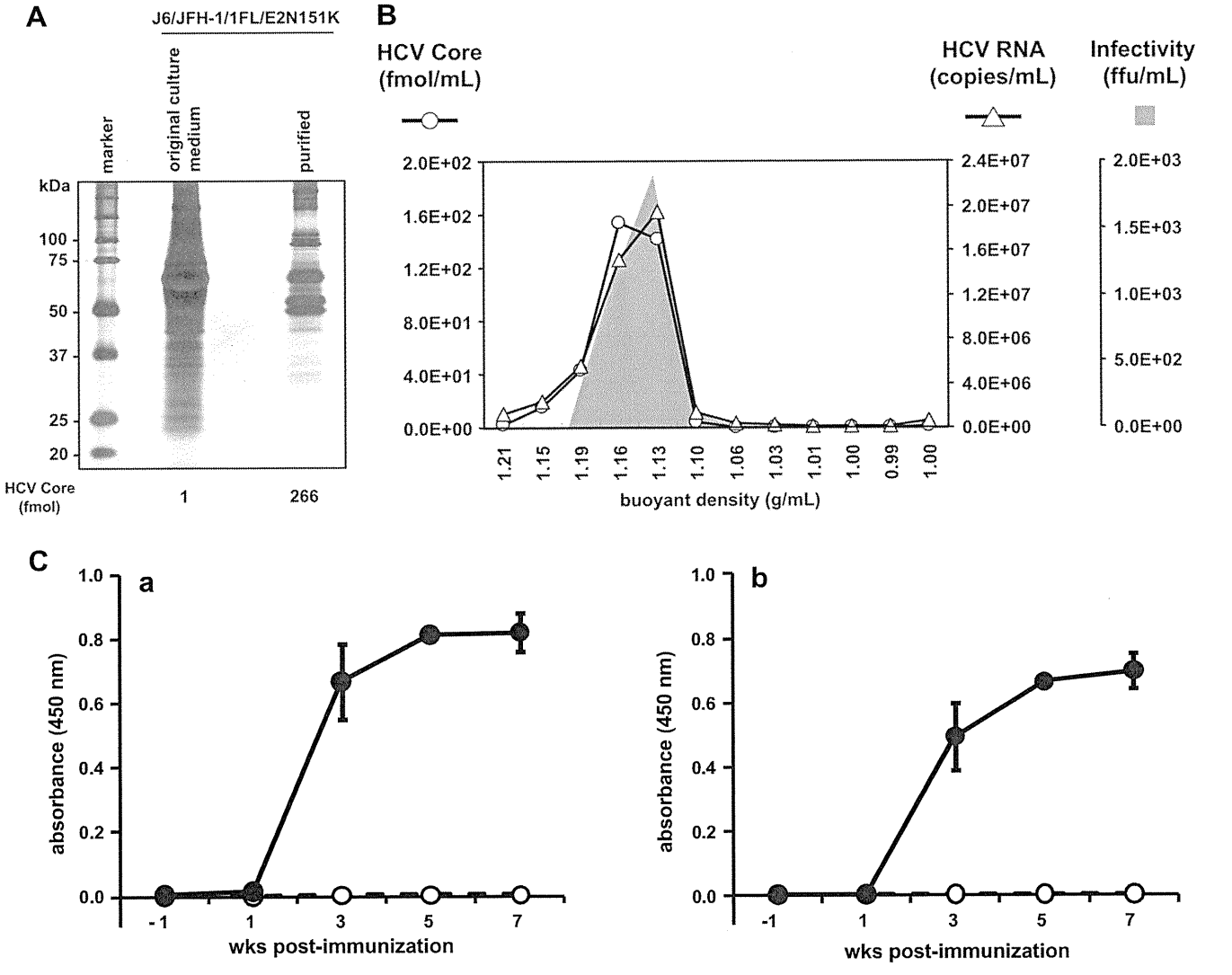

Fig. 4. Physical properties and immunogenicity of purified HCV particles. (A) Silver staining of non-purified (original culture medium) and purified HCV samples. The non-purified and purified samples contained 1 and 266 fmol, respectively, of the HCV core. (B) Sucrose density gradient analysis of purified HCV particles. The level of the HCV core protein (open circles), HCV RNA (open triangles) and the HCV infectivity towards naïve Huh-7 cells (shown in gray) were analyzed for each fraction as described in Section 2. (C) Purified HCV particles (closed circles) or saline (open circles) were intraperitoneally injected into BALB/c mice ($n = 3$), and sera were collected at the indicated times. The collected sera were examined for the presence of anti-E2 (a) and anti-FLAG (b) antibodies using the J6E2/Fc protein and the FLAG peptide as antigens in an EIA as described in Section 2.

particles were immunogenic and that insertion of a tag into the E2 protein could induce antibodies as a secondary immunogen.

4. Discussion

In this study we showed that infectious FLAG-tagged HCV particles with an N151K mutation that modulated HCV-glycosylation could be efficiently produced in cells and purified on a FLAG-agarose column. This purification procedure allowed analysis of the physical properties of the particles and the generation of anti-E2 antibodies.

The FLAG-tagged HCV particles were purified by simple anti-FLAG affinity chromatography in combination with ultrafiltration. However, the efficiency of purification was low, and the recovery of the HCV core protein in the final purified virus preparation was only approximately 5%. This low efficiency of purification of the HCV particles maybe due to a number of factors: (1) Interaction between the E2-FLAG protein and the anti-FLAG-agarose column may have been prevented by cellular host proteins with specific or non-specific affinity for the anti-FLAG-agarose, (2) A conformation change may have occurred in the E2 protein due to insertion of the FLAG sequence, which may have blocked FLAG interaction with anti-FLAG, (3) Free FLAG-E2 proteins may have bound more tightly to the FLAG-agarose than the FLAG-E2 protein on the viral surface. Nevertheless, sufficient purified FLAG-HCV particles were obtained with this purification procedure for further analysis.

In the density gradient analysis of the purified HCV particles, the peak of the HCV core protein coincided with the peaks of HCV RNA and viral infectivity. In previous reports of density gradient fractionation of non-FLAG-tagged viral particles, the peak of infectivity was reported to shift to a lighter density fraction than the peaks of HCV core protein or RNA [8,13,14]. This discrepancy between our, and previous, data may be explained by the fact that the properties of the purified FLAG-tagged HCV particles may differ from those of the JFH-1 based HCV particles reported previously. Regarding viral infectivity, it is known that cholesterol and sphingolipid association with HCV particles is important for virion maturation and infectivity [9]. The association of HCV particles with these lipids occurs in lipid rafts [9]. Since the E2-FLAG protein may have a decreased dependency on lipid rafts compared to the non-tagged E2 protein, this therefore resulted in a shift in the peak of infectivity. Alternatively, an association between HCV and very-low-density lipoprotein (VLDL) has an important role in HCV infectivity [15]. Tagging of HCV particles with FLAG may have somehow changed the association of HCV with VLDL and cause the observed shift in the infectivity peak. The mechanism of the shift of the infectivity peak of the FLAG-HCV particles needs to be examined in more detail in future studies.

HCV particles from human plasma samples have been previously examined by immunogold electron microscopy [16]. In the present study, we could clearly observe spherical particle structures of 40–60 nm in the purified samples. Furthermore, the FLAG-tagged HCV particles were aggregated by anti-FLAG antibody. This is the first report of the aggregation of HCV particles produced in an *in vitro* culture system. This method may therefore facilitate future examination of the detailed conformation of HCV particles and future elucidation of HCV particle structure by cryo-electron microscopy. However, it is regarded structural analysis as difficult to that aggregated HCV particles were inequable showing in this report because of this method also gathered defective viral particles which have the E2-FLAG protein.

Immunization of mice with purified FLAG-tagged HCV particles induced anti-E2 as well as anti-FLAG antibodies. These results indicated that the envelope proteins of the FLAG-tagged HCV particles were immunogenic and that insertion of a tag into the E2 protein could induce antibodies as a secondary immunogen. Thus, not only epitopes of viral origin, but also an epitope inserted into the virus, can induce an immune response. Although it is unclear how many amino acids can be inserted into the E2 HVR1, at least a triple FLAG-tag sequence (25 amino acids) is possible as shown in this study.

In conclusion, we have established a simple system for the purification of recombinant infectious FLAG-epitope-tagged HCV particles. The use of this system may contribute to studies aimed at a detailed analysis of HCV particle structure and towards HCV vaccine development.

Acknowledgments

This work was partially supported by a grant-in-aid for Scientific Research from the Japan Society for the Promotion of Science, from the Ministry of Health, Labor and Welfare of Japan, by the Research on Health Sciences Focusing on Drug Innovation from the Japan Health Sciences Foundation, and by the Japanese Society of Gastroenterology.

References

[1] K. Shimotohno, Hepatitis C virus as a causative agent of hepatocellular carcinoma, Intervirology 38 (1995) 162–169.
[2] Q.L. Choo, K.H. Richman, J.H. Han, K. Berger, C. Lee, C. Dong, C. Gallegos, D. Coit, R. Medina-Selby, P.J. Barr, A.J. Weiner, D.W. Bradley, G. Kuo, M. Houghton, Genetic organization and diversity of the hepatitis C virus, Proc. Natl. Acad. Sci. USA 88 (1991) 2451–2455.
[3] N. Kato, M. Hijikata, Y. Ootsuyama, M. Nakagawa, S. Ohkoshi, T. Sugimura, K. Shimotohno, Molecular cloning of the human hepatitis C virus genome from Japanese patients with non-A, non-B hepatitis, Proc. Natl. Acad. Sci. USA 87 (1990) 9524–9528.
[4] Z. Stamataki, S. Coates, M.J. Evans, M. Wininger, K. Crawford, C. Dong, Y.L. Fong, D. Chien, S. Abrignani, P. Balfe, C.M. Rice, J.A. McKeating, M. Houghton, Hepatitis C virus envelope glycoprotein immunization of rodents elicits cross-reactive neutralizing antibodies, Vaccine 25 (2007) 7773–7784.
[5] T. Kato, T. Date, M. Miyamoto, A. Furusaka, K. Tokushige, M. Mizokami, T. Wakita, Efficient replication of the genotype 2a hepatitis C virus subgenomic replicon, Gastroenterology 125 (2003) 1808–1817.
[6] T. Wakita, T. Pietschmann, T. Kato, T. Date, M. Miyamoto, Z. Zhao, K. Murthy, A. Habermann, H.G. Krausslich, M. Mizokami, R. Bartenschlager, T.J. Liang, Production of infectious hepatitis C virus in tissue culture from a cloned viral genome, Nat. Med. 11 (2005) 791–796.
[7] J. Zhong, P. Gastaminza, G. Cheng, S. Kapadia, T. Kato, D.R. Burton, S.F. Wieland, S.L. Uprichard, T. Wakita, F.V. Chisari, Robust hepatitis C virus infection in vitro, Proc. Natl. Acad. Sci. USA 102 (2005) 9294–9299.
[8] B.D. Lindenbach, M.J. Evans, A.J. Syder, B. Wolk, T.L. Tellinghuisen, C.C. Liu, T. Maruyama, R.O. Hynes, D.R. Burton, J.A. McKeating, C.M. Rice, Complete replication of hepatitis C virus in cell culture, Science 309 (2005) 623–626.
[9] H. Aizaki, K. Morikawa, M. Fukasawa, H. Hara, Y. Inoue, H. Tani, K. Saito, M. Nishijima, K. Hanada, Y. Matsuura, M.M. Lai, T. Miyamura, T. Wakita, T. Suzuki, Critical role of virion-associated cholesterol and sphingolipid in hepatitis C virus infection, J. Virol. 82 (2008) 5715–5724.
[10] M.J. van den Hoff, A.F. Moorman, W.H. Lamers, Electroporation in 'intracellular' buffer increases cell survival, Nucleic Acids Res. 20 (1992) 2902.
[11] T. Takeuchi, A. Katsume, T. Tanaka, A. Abe, K. Inoue, K. Tsukiyama-Kohara, R. Kawaguchi, S. Tanaka, M. Kohara, Real-time detection system for quantification of hepatitis C virus genome, Gastroenterology 116 (1999) 636–642.
[12] D. Delgrange, A. Pillez, S. Castelain, L. Cocquerel, Y. Rouille, J. Dubuisson, T. Wakita, G. Duverlie, C. Wychowski, Robust production of infectious viral particles in Huh-7 cells by introducing mutations in hepatitis C virus structural proteins, J. Gen. Virol. 88 (2007) 2495–2503.
[13] D. Akazawa, T. Date, K. Morikawa, A. Murayama, N. Omi, H. Takahashi, N. Nakamura, K. Ishii, T. Suzuki, M. Mizokami, H. Mochizuki, T. Wakita, Characterization of infectious hepatitis C virus from liver-derived cell lines, Biochem. Biophys. Res. Commun. 377 (2008) 747–751.
[14] Y. Miyanari, K. Atsuzawa, N. Usuda, K. Watashi, T. Hishiki, M. Zayas, R. Bartenschlager, T. Wakita, M. Hijikata, K. Shimotohno, The lipid droplet is an important organelle for hepatitis C virus production, Nat. Cell Biol. 9 (2007) 1089–1097.
[15] S.U. Nielsen, M.F. Bassendine, A.D. Burt, C. Martin, W. Pumeechockchai, G.L. Toms, Association between hepatitis C virus and very-low-density lipoprotein (VLDL)/LDL analyzed in iodixanol density gradients, J. Virol. 80 (2006) 2418–2428.
[16] M. Kaito, S. Watanabe, H. Tanaka, N. Fujita, M. Konishi, M. Iwasa, Y. Kobayashi, E.C. Gabazza, Y. Adachi, K. Tsukiyama-Kohara, M. Kohara, Morphological identification of hepatitis C virus E1 and E2 envelope glycoproteins on the virion surface using immunogold electron microscopy, Int. J. Mol. Med. 18 (2006) 673–678.

THE JOURNAL OF BIOLOGICAL CHEMISTRY VOL. 286, NO. 43, pp. 37264–37273, October 28, 2011

Role of the Endoplasmic Reticulum-associated Degradation (ERAD) Pathway in Degradation of Hepatitis C Virus Envelope Proteins and Production of Virus Particles*[S]

Received for publication, May 7, 2011, and in revised form, August 18, 2011 Published, JBC Papers in Press, August 30, 2011, DOI 10.1074/jbc.M111.259085

Mohsan Saeed[§], Ryosuke Suzuki[‡], Noriyuki Watanabe[‡], Takahiro Masaki[‡], Mitsunori Tomonaga[‡], Amir Muhammad[¶], Takanobu Kato[‡], Yoshiharu Matsuura[‖], Haruo Watanabe[§], Takaji Wakita[‡], and Tetsuro Suzuki[‡ ‡‡1]**

*From the [‡]Department of Virology II, National Institute of Infectious Diseases, Tokyo 162-8640, Japan, the [§]Department of Infection and Pathology, Graduate School of Medicine, the University of Tokyo, Tokyo 113-0033, Japan, the [¶]Department of Pathology, Khyber Girls Medical College, Peshawar 25000, Pakistan, the [‖]Research Institute of Microbial Diseases, Osaka University, Osaka 565-0871, Japan, the **National Institute of Infectious Diseases, Tokyo 162-8640, Japan, and the [‡‡]Department of Infectious Diseases, Hamamatsu University School of Medicine, Hamamatsu 431-3192, Japan*

Background: HCV causes ER stress in the infected cells.
Results: HCV-induced ER stress leads to increased expression of certain proteins that in turn enhance the degradation of HCV glycoproteins and decrease production of virus particles.
Conclusion: HCV infection activates the ERAD pathway, leading to modulation of virus production.
Significance: ERAD plays a crucial role in the viral life cycle.

Viral infections frequently cause endoplasmic reticulum (ER) stress in host cells leading to stimulation of the ER-associated degradation (ERAD) pathway, which subsequently targets unassembled glycoproteins for ubiquitylation and proteasomal degradation. However, the role of the ERAD pathway in the viral life cycle is poorly defined. In this paper, we demonstrate that hepatitis C virus (HCV) infection activates the ERAD pathway, which in turn controls the fate of viral glycoproteins and modulates virus production. ERAD proteins, such as EDEM1 and EDEM3, were found to increase ubiquitylation of HCV envelope proteins via direct physical interaction. Knocking down of EDEM1 and EDEM3 increased the half-life of HCV E2, as well as virus production, whereas exogenous expression of these proteins reduced the production of infectious virus particles. Further investigation revealed that only EDEM1 and EDEM3 bind with SEL1L, an ER membrane adaptor protein involved in translocation of ERAD substrates from the ER to the cytoplasm. When HCV-infected cells were treated with kifunensine, a potent inhibitor of the ERAD pathway, the half-life of HCV E2 increased and so did virus production. Kifunensine inhibited the binding of EDEM1 and EDEM3 with SEL1L, thus blocking the ubiquitylation of HCV E2 protein. Chemical inhibition of the ERAD pathway neither affected production of the Japanese encephalitis virus (JEV) nor stability of the JEV envelope protein. A co-immunoprecipitation assay showed that EDEM orthologs do not bind with JEV envelope protein. These findings highlight the crucial role of the ERAD pathway in the life cycle of specific viruses.

Quality control of proteins, such as the elimination of misfolded proteins, is largely connected with the endoplasmic reticulum (ER),[2] which is an organelle responsible for the folding and distribution of secretory proteins to their sites of action. This pathway is termed ER-associated degradation (ERAD) and is triggered by ER stress. It results in retrotranslocation of misfolded proteins into the cytosol, followed by polyubiquitylation and proteasomal degradation (1). Several viral infections have been reported to trigger the ERAD pathway (2–4); however, the role of this pathway in the life cycle of viruses remains poorly defined.

Initiation of the ERAD pathway occurs from the oligomerization and autophosphorylation of IRE1, an ER stress sensor. The activated IRE1 removes an intron from X-box-binding protein 1 (XBP1) mRNA, which then encodes a potent transcription factor for activation of genes, for example, ER degradation-enhancing α-mannosidase-like protein (EDEM). EDEM1 (5), along with its two homologs EDEM2 (6) and EDEM3 (7), as well as ER mannosidase I (ER ManI), belong to the glycoside hydrolase 47 family. EDEMs are thought to function as lectins that deliver misfolded glycoproteins to the ERAD pathway. However, the precise mechanism by which they assist in glycoprotein quality control remains unclear.

Hepatitis C virus (HCV) infection is a major cause of chronic liver disease. The RNA genome of HCV, a member of the Fla-

* This work was supported by grants-in-aid from the Ministry of Health, Labor and Welfare, and from the Ministry of Education, Culture, Sports, Science, and Technology, Japan.
[S] The on-line version of this article (available at http://www.jbc.org) contains supplemental Figs. S1–S7.
[1] To whom correspondence should be addressed: Dept. of Infectious Diseases, Hamamatsu University School of Medicine, Hamamatsu 431-3192, Japan. Tel.: 81-53-435-2336; Fax: 81-53-435-2338; E-mail: tesuzuki@hama-med.ac.jp.

[2] The abbreviations used are: ER, endoplasmic reticulum; CHX, cycloheximide; EDEM, ER degradation-enhancing α-mannosidase-like protein; ERAD, ER-associated degradation; HCV, hepatitis C virus; JEV, Japanese encephalitis virus; KIF, kifunensine; ManI, mannosidase I; m.o.i., multiplicity of infection; TM, tunicamycin; XBP1, X-box-binding protein 1; IRE, inositol-requiring enzyme.

viviridae family, encodes the viral structural proteins Core, E1, E2, and p7, as well as six nonstructural proteins (8, 9). Two *N*-glycosylated envelope proteins E1 and E2 are exposed on the surface of the virus and are necessary for viral entry.

The aim of this study was to investigate whether the ERAD pathway is activated upon HCV infection and whether this affects the quality control of virus glycoproteins and virion production. We show that HCV infection triggers the ERAD pathway, possibly through IRE1-mediated splicing of XBP1. Moreover, EDEM1 and EDEM3, but not EDEM2, interact with HCV glycoproteins, resulting in increased ubiquitylation. EDEM1 knockdown and chemical inhibition of the ERAD pathway increases glycoprotein stability, as well as production of infectious virus particles, whereas overexpression of EDEM1 decreases virion production. These results provide insight into the mechanism by which HCV triggers the ERAD pathway and subsequently affects the quality control of virus glycoproteins and virus particle production.

EXPERIMENTAL PROCEDURES

Cell Culture and Chemicals—Human hepatoma cells HuH-7 and HuH-7.5.1 (a gift from Dr. F. V. Chisari (The Scripps Research Institute) (10) and human embryonic kidney cells 293T were cultured at 37 °C and 5% CO_2 in DMEM containing 10% FBS, 10 mM HEPES, 1 mM sodium pyruvate, nonessential minimum amino acids, 100 units/ml penicillin, and 100 μg/ml streptomycin. Tunicamycin (TM) was purchased from Sigma-Aldrich, and kifunensine (KIF) was purchased from Toronto Research Chemicals (Ontario, Canada).

Preparation of Virus Stock—HCV JFH-1 was generated by introducing *in vitro* transcribed RNA into HuH-7.5.1 cells by electroporation, and virus stocks were prepared by infecting at a multiplicity of infection (m.o.i.) of 0.01, as described previously (10). Infected cells were grown in culture medium containing 2% FBS, and supernatants were collected after multiple passages to get high titer virus. The supernatants were concentrated using a 500-kDa hollow fiber module (GE Healthcare) resulting in ~90% recovery of the virus. Focus-forming units were measured with an anti-HCV core antibody to determine virus titration (2H9, described below). Virus stocks containing 1×10^7 focus-forming units/ml were divided into small aliquots and stored at −80 °C until use. rAT strain of Japanese encephalitis virus (JEV) (11) was used to generate virus stock.

Plasmids—cDNAs of mouse EDEM1-HA, EDEM2, and EDEM3-HA, having 92, 93, and 91% amino acid homology with their human orthologs, respectively, were a kind gift from Drs. N. Hosokawa (Kyoto University) and K. Nagata (Kyoto Sangyo University). A HA tag was attached to the C terminus of EDEM2 by PCR, and sequencing analysis was performed to confirm the sequence. To generate pJFH/E1dTM-myc and pJFH/E2dTM-myc, HCV E1 encoding amino acids 170–352 and HCV E2 encoding amino acids 340–714 of JFH-1 polyprotein were amplified by PCR with forward primer and reverse primer containing NotI and XbaI restriction sites, respectively, and cloned into a NotI/XbaI site of the pEF1/Myc-His plasmid (Invitrogen). The pCAGC105E plasmid carrying PrM and E proteins of the rAT strain of JEV has been described (12). Plasmids carrying the firefly luciferase reporter gene under control of the intact promoter of GRP78 and GRP94 or the defective promoter lacking ERSE elements have been described (13) and were a kind gift from Dr. K. Mori (Kyoto University).

Antibodies—Rabbit polyclonal antibodies included anti-HA (Sigma-Aldrich), anti-HCV NS5A (14), anti-SEL1L (Sigma-Aldrich), anti-ubiquitin (MBL, Nagoya, Japan), and anti-JEV E antibodies. The mouse monoclonal antibodies were anti-HA (clone 16B12; Covance, Emeryville, CA), anti-HCV E2 (clone 8D10-3),[3] anti-β-actin (clone AC15; Sigma-Aldrich), anti-HCV core (clone 2H9) (15), and anti-Myc (clone 9E10; Santa Cruz Biotechnology, Santa Cruz, CA) antibodies. Anti-JEV antibodies have been described (16) and were a kind gift from Drs. C. K. Lim and T. Takasaki (National Institute of Infectious Diseases).

Analysis of XBP1 Splicing—Total RNA was extracted from cells using Isogen (Nippon Gene, Tokyo, Japan) following the manufacturer's protocol, and 2 μg of RNA was subjected to cDNA synthesis using oligo(dT) and Superscript III (Invitrogen). PCR was carried out using specific primers 5′-AAACAGAGTAGCAGCTCAGACTGC-3′ and 5′-GTATCTCTAAGACTAGGGGCTTGGTA-3′ for XBP1 and 5′-TCCTGTGGCATCCACGAAACT-3′ and 5′-GAAGCATTTGCGGTGGACGAT-3′ for β-actin to generate PCR fragments of 598 bp for unspliced XBP1, 572 bp for spliced XBP1, and 315 bp for β-actin. The following cycling conditions were used to amplify the genes: 1 cycle of 98 °C for 3 min, followed by 30 cycles of 98 °C for 20 s, 55 °C for 30 s, and 72 °C for 1 min, followed by a final extension of 72 °C for 10 min. The PCR product of XBP1 was further digested with PstI enzyme (New England Biolabs) and resolved on a 2% agarose gel prepared in TAE buffer. Unspliced XBP1 yielded two smaller fragments of 291 and 307 bp whereas spliced XBP1 stayed intact due to loss of the restriction site after splicing.

Gene Microarray Analysis—For microarray analysis, RNA was extracted from HuH-7.5.1 cells at 48 and 72 h after JFH-1 infection. Cells treated for 12 h with 5 μg/ml TM served as a positive control. Hybridization was performed on a 3D-Gene (see 3D-Gene web site) Human Oligonucleotide chip 25k (Toray Industries Inc., Tokyo, Japan). For efficient hybridization, this microarray chip has three dimensions and is constructed with a well between the probes and cylinder stems with 70-mer oligonucleotide probes on the top. Total RNA was labeled with Cy3 or Cy5 using the Amino Allyl MessageAMP II aRNA Amplification kit (Applied Biosystems). The Cy3- or Cy5-labeled aRNA pools were subjected to hybridization for 16 h using the supplier's protocol. Hybridization signals were scanned using a ScanArray Express Scanner (PerkinElmer Life Sciences) and processed by GenePixPro version 5.0 (Molecular Devices, Sunnyvale, CA). Detected signals for each gene were normalized using a global normalization method (Cy3/Cy5 ratio median = 1). Genes with Cy3/Cy5 normalized ratios $>\log_2 1.0$ or $<\log_2 -1.0$ were defined, respectively, as significantly up- or down-regulated genes.

Quantification of Cellular Gene Expression—Gene expression levels were measured using predesigned assay-on-demand (Applied Biosystems). RT-PCR amplification was performed

[3] D. Akazawa, N. Nakamura, and T. Wakita, unpublished data.

under the following conditions: 48 °C for 30 min, 95 °C for 10 min, 50 cycles of 95 °C for 15 s, and 60 °C for 1 min. Standard curves were constructed on a 1:5 serial dilution of the RNA template. The results were normalized to GAPDH mRNA levels.

Determination of Protein Stability—HuH-7 cells were infected with HCV JFH-1 at a m.o.i. of 2. Six hours after infection, the cells were either treated with KIF or transfected with EDEM1 siRNA. Forty hours later, culture medium was replaced with 100 μg/ml cycloheximide (CHX). Cells, including floating cells, were harvested at different time points after CHX addition, and immunoblotting was performed to determine the amount of HCV E2.

Plasmid Transfection and Immunoprecipitation—HuH-7 or 293T cells were seeded in 6-well cell culture plates at 3×10^5 cells/well and cultured overnight. Plasmid DNA was transfected into cells using TranIT-LT1 transfection reagent (Mirus, Madison, WI). Cells were harvested at 48 h after transfection, washed once with 1 ml of PBS, and lysed in 200 μl of lysis buffer (20 mM Tris-HCl, pH 7.4, 135 mM NaCl, 1% Triton X-100, and 10% glycerol supplemented with 50 mM NaF, 5 mM Na_3VO_4, and protease inhibitor mixture tablets (Roche Diagnostics). Cell lysates were sonicated at 4 °C for 10 min, incubated for 30 min at 4 °C, and centrifuged at 14,000 × *g* for 5 min at 4 °C. After preclearing for 2 h, the supernatants were immunoprecipitated overnight by rotating with 1.5 μl of anti-HA monoclonal antibody (16B12) or anti-HCV E2 monoclonal antibody (clone 8D10-3) at 4 °C. The immunocomplexes were then captured on protein G-agarose beads (Invitrogen) by rotation-incubation at 4 °C for 3 h. Beads were subsequently precipitated by centrifugation at 800 × *g* for 1 min and washed five times with lysis buffer. Finally, proteins bound to the beads were boiled in 40 μl of SDS sample buffer and subjected to SDS-PAGE.

Western Blotting—Proteins resolved by SDS-PAGE were transferred onto PVDF membranes (Immobilon; Millipore). After blocking in 2% skim milk, the membranes were probed with primary antibodies followed by exposure to peroxidase-conjugated secondary antibodies and visualization with an ECL Plus Western blotting detection system (GE Healthcare). The intensity of the bands was measured using a computerized imaging system (ImageJ software; National Institutes of Health).

Small Interfering RNA (siRNA) Transfection—HuH-7 cells were transfected with duplex siRNAs at a final concentration of 10 nM using Lipofectamine RNAiMAX (Invitrogen). Three siRNAs for each gene were examined for knock-down efficiency and cytotoxic effects. The siRNA with best performance was selected for further experiments. Target sequences of the siRNAs which exhibited the best knock-down efficiencies were as follows: EDEM1 (sense) 5′-CAUAUCCUCGGGUGAAUCUtt-3′, EDEM2 (sense) 5′-GAAUGUCUCAGAAUUCCAAtt-3′, EDEM3 (sense) 5′-CAUGAGACUACAAAUCUUAtt-3′, IRE1 (sense) 5′-GGACGUGAGCGACAGAAUAtt-3′. 5′-GGUGUCCUUACCAUACUAAtt-3′ served as a negative control. The lowercase letters denote overhanging deoxyribonucleotides.

Quantification of HCV Core and RNA—HCV core was quantified using an enzyme immunoassay (Ortho HCV antigen ELISA kit; Ortho Clinical Diagnostics, Tokyo, Japan). HCV RNA was quantified as described (17).

Statistical Analysis—Student's *t* test was employed to calculate the statistical significance of the results. $p < 0.05$ was considered significant.

RESULTS

HCV Infection Induces XBP1 mRNA Splicing and EDEM Expression—XBP1 plays a key role in activating the ERAD pathway, which mediates unfolded protein response in the ER. Under conditions of ER stress, XBP1 mRNA is processed by unconventional splicing and translated into functional XBP1, which in turn mediates transcriptional up-regulation of a variety of ER stress-dependent genes. The resultant activation of downstream pathways boosts the efficiency of ERAD, which coincides with elevated transcription of EDEMs. To validate our method for detecting activation of the ERAD pathway, we exposed HuH-7.5.1 cells to TM, which is a typical ER stress inducer, and performed an assay to quantify spliced XBP1 mRNA, as described under "Experimental Procedures," at different time points after treatment. The spliced form of XBP1 mRNA started accumulating within these cells as early as 2 h after exposure to TM (Fig. 1*A*), and levels remained elevated until at least 12 h after treatment. Quantitative RT-PCR showed that mRNA levels of EDEM1, EDEM2, and EDEM3 were elevated in TM-treated cells whereas ER ManI, which is not an ER stress-responsive gene, did not show any up-regulation (Fig. 1*B*). To examine involvement of the ERAD pathway in the HCV life cycle, we infected HuH-7.5.1 cells with JFH-1 at m.o.i. of 5 and analyzed XBP1 mRNA splicing and EDEM up-regulation. Upon infection, the fragment corresponding to spliced XBP1 mRNA, was detectable 8 h after infection, and the difference in splicing between mock- and HCV-infected cells became more pronounced at 48 h after infection and then persisted (Fig. 1*C*). Increased levels of XBP1 mRNA splicing were dependent on the m.o.i. (supplemental Fig. 1*A*), suggesting that expression of active XBP1 was induced by HCV infection. A small amount of spliced XBP1 was detected in mock-infected cells, presumably because of some intrinsic stress. A 3.1-fold increase in the level of EDEM1 mRNA was observed at 3–4 days after infection ($p < 0.05$). Increases in EDEM2 and EDEM3 mRNA levels were moderate and reached ~1.5-fold, whereas ER ManI mRNA exhibited no change after infection (Fig. 1*D*). Expression of EDEMs, particularly EDEM1, was up-regulated in accordance with HCV infection titers (supplemental Fig. 1*B*). Knocking down the IRE1 gene (Fig. 1*E*) effectively reversed the accumulation of spliced XBP1, as well as the transcriptional up-regulation of EDEM1 (Fig. 1*F*), thus confirming that HCV infection induces ERAD through the IRE1-XBP1 pathway.

To enable a comprehensive investigation of the transcriptional changes that occur, up- and down-regulation of the transcriptome was examined in HCV-infected cells and in TM-treated cells. The results were compared with those of mock-transfected cells at each time point. A range of genes involved in ER stress was found to be regulated in HCV-infected and in TM-treated cells (Fig. 2*A*). EDEM1 was signifi-

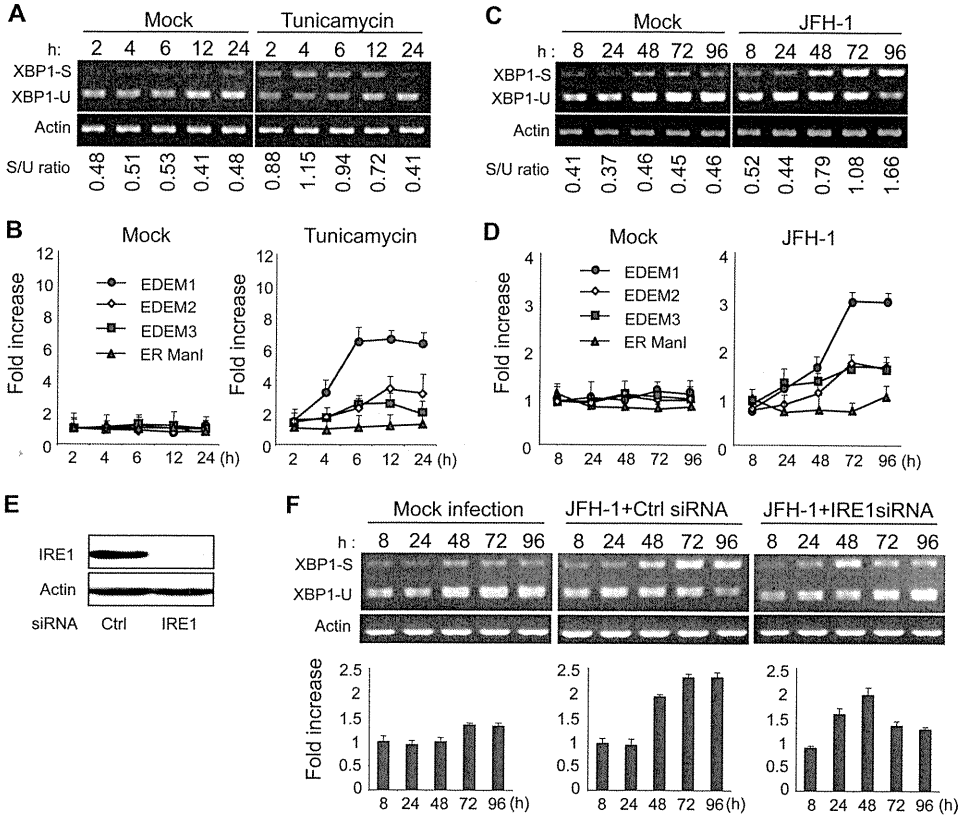

FIGURE 1. **Splicing of XBP1 mRNA and induction of ERAD gene expression in HCV JFH-1-infected cells.** *A*, splicing of XBP1 mRNA analyzed in mock- and TM (5 μg/ml)-treated HuH-7.5.1 cells at different time points after treatment. The *upper* and *lower bands* represent spliced and unspliced RNA, respectively. The *numbers* at the *bottom* of the *panel* indicate the density ratios of bands corresponding to spliced and unspliced XBP1. *B*, graphs showing the -fold induction of EDEM1, EDEM2, EDEM3, and ER Man1 mRNA in HuH-7.5.1 cells treated or untreated with TM. Data are normalized to GAPDH expression levels. The mean ± S.D. (*error bars*) of three independent experiments are shown. *C*, splicing of XBP1 mRNA analyzed in mock- and HCV JFH-1-infected HuH-7.5.1 cells (m.o.i. 5) at different time points after infection. *Numbers* at the *bottom* of the *panel* indicate the density ratios of bands corresponding to spliced and unspliced XBP1. *D*, real-time PCR analysis of EDEM1, EDEM2, EDEM3, and ER ManI mRNA induction in mock- and HCV-infected cells. Data are normalized to GAPDH expression. The mean ± S.D. of three independent experiments are shown. Note that a reduction in the level of GAPDH mRNA within infected cells was not observed until 96 h after infection when a slight decrease was observed. This led us to use GAPDH as a housekeeping gene in our experiments. *E*, Western blotting of IRE1 in cells transfected with mock or gene-specific siRNA of IRE1. *F*, splicing of XBP1 mRNA and induction of EDEM1 in HCV-infected cells after knocking down of the IRE1 gene. HuH-7.5.1 cells infected with JFH-1 at a m.o.i. of 5 were transfected with mock (*center*) or IRE1-specific siRNA (*right*) 48 h after infection, after which splicing of XBP1 (*upper*) and transcriptional up-regulation of EDEM1 (*lower*) were examined at the indicated time points after infection. The mean ± S.D. of two independent experiments are shown.

cantly up-regulated upon HCV infection, whereas expression levels of EDEM2 and EDEM3 remained unchanged. Although transcriptional changes caused by HCV infection in many of the genes listed are analogous to those that occur in cells treated with TM, up-regulation of two ER chaperone proteins, GRP78 and GRP94, was induced by TM treatment but not by HCV infection. This differential induction was confirmed by a reporter assay for GRP78 promoter and GRP94 promoter activities (Fig. 2*B*). These results are in agreement with a previously described finding that GRP78 and GRP94 are not responsive to HCV infection in hepatoma cells (18). It remains likely that HCV infection interferes with transcriptional activation of some ER chaperone proteins; however, the mechanism by which this occurs remains to be elucidated.

EDEMs Cause Ubiquitylation of HCV Glycoproteins and Enhance Their Degradation—Because EDEMs have been reported to enhance proteasomal degradation of ERAD substrates through direct binding, we investigated the interaction of EDEMs with HCV glycoproteins in 293T cells by co-transfecting the expression plasmids for E1dTM or E2dTM together with plasmids carrying either EDEM or ER ManI genes. Immunoprecipitation and immunoblotting demonstrated that each EDEM, but not ER ManI, was capable of interacting with E2 (Fig. 3*A*) and E1 (supplemental Fig. S2). HCV glycoproteins displayed enhanced mobility when co-expressed with EDEM1, EDEM3, or ER ManI, which could be due to the mannosidase activity of these proteins, which is lacking in EDEM2 (6). HCV primarily replicates in hepatocytes so we examined the interaction of EDEMs with E2dTM in HuH-7 cells as well, which yielded similar results (data not shown). E2dTM lacks the transmembrane domain, which could affect its folding and ER retention and thus modulate the ability of this protein to interact with EDEMs and ER ManI. Second, E1 and E2 glycoproteins assemble as noncovalent heterodimers to make functional complexes, which may alter the interaction of these proteins with EDEMs. To address these issues, we co-transfected HuH-7 cells with plasmids carrying full-length E1E2 glycoproteins together with plasmids carrying either EDEMs or ER ManI. Similar phenotypes were produced following transfection full-length E1E2 proteins (supplemental Fig. S3*A*), demonstrating that functional complexes of HCV glycoproteins bind with EDEMs. Recently, we have reported on the development of a